NDRG2 Regulates Adherens Junction Integrity to Restrict Colitis and Tumorigenesis

Yongzheng Ma[1,§], Mengying Wei[1,§], Liangliang Shen[1,§], Yuqiao Xu[2,§], Lijun Liu[1], Xin Bu[1], Hongyan Qin[3], Zengshan Li[2], Zhe Wang[2], Kaichun Wu[4], Libo Yao[1], and Jian Zhang[1,5*]

[1]The State Key Laboratory of Cancer Biology, Department of Biochemistry and Molecular Biology, the Fourth Military Medical University, Xian 710032, China;

[2]The State Key Laboratory of Cancer Biology, Department of Pathology, the Fourth Military Medical University, Xian 710032, China;

[3]State Key Laboratory of Cancer Biology, Department of Medical Genetics and Developmental Biology, Fourth Military Medical University, Xian 710032, China;

[4]State Key Laboratory of Cancer Biology, Xijing Hospital of Digestive Disease, Xijing Hospital, The Fourth Military Medical University, Xian 710032, China.

[5]Key Laboratory of Gastrointestinal Pharmacology of Chinese Materia Medica of the State Administration of Traditional Chinese Medicine, Xi'an 710032, China;

[*]**Correspondence:** Jian Zhang, MD, PhD, The State Key Laboratory of Cancer Biology, Department of Biochemistry and Molecular Biology, the Fourth Military Medical University, Xi'an, China. Email: biozhangj@fmmu.edu.cn; fax: (86) 29-8477 3947.

[§]These authors contributed equally to this work.

Conflicts of interest: The authors have declared that no conflict of interest exists.

Abstract

Inflammatory bowel disease (IBD) is a multifactorial chronic inflammatory disease, which may further develop into colitis-associated cancer (CAC) with the increasing morbidity. Although the mechanism of IBD is not fully understood, it's well-recognized that adherens junction (AJ) plays an important role in gut homeostasis and pathogenesis of IBD. Our group firstly reported N-Myc downstream-regulated gene 2 (NDRG*2*) as a novel tumor suppressor gene. Much evidences showed that NDRG2 inhibited colorectal cancer proliferation and metastasis. However, whether NDRG2 affects colitis initiation and colitis-associated cancer is unclear. In this study, we found that *Ndrg2* deficiency aggravates colitis initiation and colitis-associated tumor development using an intestine-specific *Ndrg2* knockout mouse. We proved the novel mechanism that N-terminal region of NDRG2 enhanced the interaction of E3 ligase FBXO11 with Snail, the repressor of E-cadherin, to promote Snail ubiquitination and degradation. And *Ndrg2* loss led to AJ structure destruction *via* E-cadherin reduction, resulting in diminished epithelial barrier function and enhanced gut permeability. Furthermore, in human IBD patients, NDRG2 was positively correlated with E-cadherin expression, whereas negatively correlated with inflammation degree and Snail expression. Thus, our study has revealed that NDRG*2* is an essential intestinal epithelial barrier regulator and plays important roles in gut homeostasis maintenance and colitis-associated tumor development.

Introduction

Inflammatory bowel disease (IBD) is a multifactorial chronic inflammatory disease mainly comprising Crohn's disease (CD) and ulcerative colitis (UC) that causes intestinal epithelial cell injury and relapsing chronic pathogenic rectal and colonic inflammation(1, 2). The processes of IBD initiation and progression are complicated and can be attributed to microbiome-induced imbalances in innate and adaptive immune system function and pro- and anti-inflammatory cytokine production(3, 4).

Intestinal epithelial homeostasis plays an important role in the intestinal tract. This homeostasis is maintained by a mucosal barrier, an epithelial barrier and the lamina propria(5). The mucosal barrier is regulated primarily by antimicrobial peptides and mucins to prevent bacterial penetration(6). Tight junctions (TJs), adherens junctions (AJs) and desmosomes are the main epithelial cell-to-cell connections and maintain bacteria-host homeostasis(7, 8). TJs and AJs form epithelial barriers and intercellular space seals on the colonic luminal surface, modulating gut permeability and regulating water, nutrient and large molecule transport. TJ dysfunction results in epithelial barrier disruption, increased epithelial permeability, and enhanced inflammation(9, 10).

Adherent junctions (AJs) are cell-cell adhesion complexes that participate in embryogenesis and tissue homeostasis. F-actin, p120 catenin and α-catenin are the main components of cytoplasmic plaques, while E-cadherin connects adjacent cell membranes(11). E-cadherin or p120-catenin loss results in embryonic death(2). Previous studies demonstrated that AJ dysfunction is associated with IBD and E-cadherin expression attenuation could obviously aggravate colitis, possibly due to increase of colonic epithelial barrier permeability(12, 13).

We previously identified N-myc downstream regulated gene 2 (NDRG2) as a novel tumor suppressor gene that played a role in regulating the proliferation, differentiation, apoptosis and metastasis of multiple types of malignant tumors(14-17). Consistent with this finding, NDRG2 down-regulation has been observed in multiple human cancer cell lines and tumors, especially colorectal carcinoma(18-20). Notably, our recent data showed that NDRG2 could inhibit colorectal carcinoma cell proliferation and promote colorectal carcinoma cell differentiation(21). Interestingly, we found that decreased NDRG2

expression was a powerful and independent predictor of a poor prognosis in colorectal cancer and was associated with poor 5-year survival rates and relapse(22, 23). Furthermore, NDRG2 can inhibit epithelial–mesenchymal transition (EMT) by positively regulating E-cadherin expression(23). However, whether NDRG2 participates in E-cadherin-mediated intestinal epithelial homeostasis remains unknown.

In this study, we generated intestine-specific conditional *Ndrg2* knockout mice and examined the roles of *Ndrg2* in AJ structure and permeability regulation in the setting of experimentally induced colitis. Furthermore, we characterized the detailed function and mechanism of NDRG2 in intestinal epithelial inflammation and evaluated the effects of *Ndrg2* deficiency on gut inflammation and colitis-associated tumor.

Results

Intestinal Ndrg2 loss aggravated colitis initiation. To explore whether NDRG2 involves the colitis process, we treated the mice with DSS and LPS respectively to mimic the colitis in vivo. We found that the endogenous NDRG2 protein level was significantly decreased in intestinal epithelial cells (IECs) isolated from mice treated with DSS and LPS respectively (Supplementary Figure 1A, B). To further determine the role of NDRG2 in colitis initiation, we generated intestine-specific conditional *Ndrg2* knockout mice featuring intestinal epithelial cells lacking *Ndrg2.* Floxed *Ndrg2* alleles were disrupted using *Cre* recombinase under the control of the *Villin*-promoter (Vil-cre) to generate intestine-specific *Ndrg2* knockout mice (*Ndrg2*$^{-/-}$) (Supplementary Figure 1C)(21). There was no difference in growth retardation between *Ndrg2*$^{-/-}$ mice and WT mice (Supplementary Figure 1D). NDRG2 expression was specifically and completely abolished in the IECs of *Ndrg2*$^{-/-}$ mice (Figure 1A, B and Supplementary Figure 1E).

To determine the role of NDRG2 in colitis initiation and progression, we induced colitis in WT and *Ndrg2*$^{-/-}$ mice on a C57/BL6 background using DSS. We found that *Ndrg2*$^{-/-}$ mice exhibited increased body weight loss compared with WT mice (Figure 1C), as well as more severe colonic shortening than their counterparts (Figure 1D, E). For histological analysis, the middle and distal colon were obtained and segmented. WT mice exhibited only mild colitis, while *Ndrg2*$^{-/-}$ mice exhibited severe colitis characterized by profound epithelial structural damage and robust

inflammatory cell infiltration (Figure 1F), as well as higher Disease Activity Index (DAI) scores (Figure 1G). Alternatively, we observed the similar results with more severe inflammation of *Ndrg2*$^{-/-}$ mice in TNBS-induced colitis model (Supplementary Figure 2A, B). For survival analysis, both WT and *Ndrg2*$^{-/-}$ mice were treated with 4% DSS for 7 days before being transitioned to DSS-free water and were counted daily. *Ndrg2*$^{-/-}$ mice exhibited increased susceptibility to lethal colitis induction compared with WT mice (Figure 1H). Taken together, our data demonstrated that intestine-specific *Ndrg2* deficiency could obviously promote colitis initiation.

Intestinal Ndrg2 Deficiency Promoted Inflammatory cell infiltration and chemokine expression. Inflammatory cell infiltration plays an important role in both UC and CD. To characterize the role of NDRG2 in colonic inflammation, WT and *Ndrg2*$^{-/-}$ mice were treated with 3% DSS for 5 days and DSS-free water for an additional 5 days. On day 10, IECs and lamina propria cells (LPCs) were isolated from WT and *Ndrg2*$^{-/-}$ mice, and combined for inflammatory cell quantification *via* flow cytometry. We noticed that DSS-free *Ndrg2*$^{-/-}$ mice exhibited slight increases in monocyte and macrophage infiltration compared with DSS-free WT mice, although the difference between the two groups was no significance (Figure 2A, B). However, DSS-treated *Ndrg2*$^{-/-}$ mice exhibited significantly increased monocyte, macrophage and neutrophil infiltration compared with WT mice subjected to the same treatment, but no change in eosinophil infiltration (Figure 2A, C). IECs were subjected to quantification analysis by qRT-PCR to determine the levels of C-C motif chemokine ligand 5 (CCL5) and C-X-C motif chemokine ligand 1/2 (CXCL1/2) expression. DSS-free *Ndrg2*$^{-/-}$ mice exhibited slightly increased chemokine expression (Figure 2D), while DSS-treated *Ndrg2*$^{-/-}$ mice exhibited dramatically increased CCL5 and CXCL1/2 expression (Figure 2D). These findings indicated that intestinal *Ndrg2* deficiency facilitated inflammatory cell recruitment by up-regulating CCL5 and CXCL1/2 expression, thereby aggravating DSS-induced colitis.

Simultaneously, cytokines regulate the balance between pro- and anti-inflammation in IBD and also play important roles in colitis progression. Thus, we detected the mRNA expression levels of the major cytokines involved in IEC inflammation in DSS-treated *Ndrg2*$^{-/-}$ and WT mice. The mRNA expression levels of several inflammation markers,

including *IL-1β*, *IL-6* and *TNF-α* (tumor necrosis factor alpha), were significantly increased in DSS-treated *Ndrg2*$^{-/-}$ mice compared with DSS-treated WT mice (Figure 2E, Supplementary Figure 3A). In contrast, the mRNA expression level of the anti-inflammatory cytokine *IL-10* was attenuated in DSS-treated *Ndrg2*$^{-/-}$ mice compared with DSS-treated WT mice (Figure 2E), while the expression of *TGF-β* was comparable between the two groups (Supplementary Figure 3B). Interestingly, there were no differences in the expression levels of *IL-12* and *IL-17*, which participate in T cell differentiation(24), between DSS-treated *Ndrg2*$^{-/-}$ and WT mice (Supplementary Figure 3C, 3D), suggesting that T cell function is not affected by intestinal *Ndrg2* deletion. Moreover, the expression level of *IL-22*, an important cytokine involved in epithelial regeneration(25), was similar between the two groups (Supplementary Figure 3E). Thus, intestinal *Ndrg2* loss aggravated DSS-induced colitis by promoting pro-inflammatory cytokine expression without affecting T cell differentiation or colonic epithelial regeneration.

Intestine-specific Ndrg2 deficiency increased LPS permeability. Lipopolysaccharide (LPS) is the main microflora-derived toxin that induces gut epithelial inflammation. We therefore examined serum LPS levels in *Ndrg2*$^{-/-}$ and WT mice treated with and without DSS. We found that there was no difference in serum LPS levels between untreated *Ndrg2*$^{-/-}$ and WT mice. However, DSS-treated *Ndrg2*$^{-/-}$ mice exhibited increased serum LPS levels compared with DSS-treated WT mice (Figure 3A).

We hypothesized that the enhanced inflammation in *Ndrg2*$^{-/-}$ mice were associated with increases in LPS permeability. So we subsequently examined whether *Ndrg2* deficiency facilitated LPS-induced inflammation. First, we determined whether LPS induced colonic epithelial inflammation in a dose-dependent manner as reported previously. After 1 week of 1 g/mL ampicillin treatment, we treated WT mice with 0.1 mg/kg and 1 mg/kg LPS for 4 hours respectively. PBS was used as a control. Then, we isolated IECs for analysis and found that LPS induced significant inflammation characterized by dose-dependent increases in the levels of IL-1β, TNF-α, and IL-6 expression, as well as dose-dependent increases in the levels of CXCL1/2 expression (Supplementary Figure 4 A-E). Then, we treated WT and

Ndrg2$^{-/-}$ mice with 0.1 mg/kg LPS for 4 hours after ampicillin treatment, detected serum LPS levels, and isolated IECs from both groups for further analysis. We found that *Ndrg2*$^{-/-}$ mice exhibited increased LPS permeability compared with WT mice (Figure 3B) and *Ndrg2* deficiency increased IL-1β, TNF-α, IL-6, CXCL-1 and CXCL-2 expression (Figure 3C, D), suggesting the enhanced inflammatory response. These data suggested that intestine-specific *Ndrg2* deficiency increased LPS permeability and promoted LPS-induced inflammation, resulting in colitis development in *Ndrg2*$^{-/-}$ mice.

Intestinal Ndrg2 loss disrupted the adherens junction integrity of normal epithelium and increased colonic permeability. Epithelial barrier dysfunction increases gut permeability and aggravates the inflammatory response in IBD. Previous studies have verified that TJ and AJ dysregulation promotes chemically induced colitis similar to IBD(26), and our previous work demonstrated that NDRG2 inhibits epithelial–mesenchymal transition (EMT) by regulating E-cadherin(23).

To further investigate the role of *Ndrg2* in DSS-induced colitis, we examined gut permeability in WT and *Ndrg2*$^{-/-}$ mice treated with or without DSS *via* FITC-dextran analysis. Untreated *Ndrg2*$^{-/-}$ mice exhibited slightly increased permeability compared with untreated WT mice (Figure 4A). The other groups of *Ndrg2*$^{-/-}$ and WT mice were treated with DSS for 5 days, and gut permeability was evaluated five days later. With the treatment of both low molecular weight Dextran (40 KD) and high molecular weight Dextran (500 KD), the DSS-treated *Ndrg2*$^{-/-}$ mice exhibited dramatically increased permeability compared with WT mice subjected to the same treatment (Figure 4A), possibly due to epithelial barrier destruction. We further examined whether the epithelial barrier was damaged in *Ndrg2*$^{-/-}$ mice with electron microscopy. Notably, compared with WT mice, *Ndrg2*$^{-/-}$ mice exhibited significant adherens junction (AJ) structural disruption but virtually no TJ structural altreation (Figure 4B). AJ distance were remarkably increased in the intestinal epithelium of *Ndrg2*$^{-/-}$ mice compared with those of WT mice (Figure 4C).

E-cadherin is a key component of AJ structure and reduced E-cadherin aggravates DSS-induced colitis(12, 27). So, we examined whether AJ destruction in the *Ndrg2*$^{-/-}$ epithelium was caused by attenuated E-cadherin expression. As expected, immunofluorescence analysis showed that

E-cadherin expression was significantly decreased in the colonic epithelium of *Ndrg2*$^{-/-}$ mice compared with WT mice (Figure 4D), suggesting that *Ndrg2* loss resulted in E-cadherin down-regulation. With western blotting analysis, E-cadherin attenuation was also demonstrated in the IECs of *Ndrg2*$^{-/-}$ mice. While, one of the key transcriptional repressor of E-cadherin, expression of Snail was significantly increased (Figure 4E). We also confirmed the alteration of E-cadherin and Snail in colorectal cancer cells HT-29 and Caco-2 with NDRG2 knockdown (Supplementary Figure 5A, 5B). These findings demonstrated that *Ndrg2* deletion disrupts AJ structure integrity in the colonic epithelium by suppressing E-cadherin expression *via* Snail up-regulation, thus increasing colonic permeability in *Ndrg2*$^{-/-}$ mice.

NDRG2 augmented E-cadherin expression via promoting the ubiquitylation and degradation of Snail. To further understand why NDRG2 loss caused E-cadherin reduction, by subjecting different FLAG-tagged NDRG2 truncations (Figure 5A, right panel), we compared the expression difference of Snail. The data demonstrated that Snail protein expression was significantly decreased with full length NDRG2 (NDRG2/FL), but abolished by NDRG2 N-terminal deletion (NDRG2/ΔN) (Figure 5A), suggesting the key role of N-terminal of NDRG2 for Snail regulation. Then we employed cycloheximide (CHX), an inhibitor of protein biosynthesis to determine the protein stability of Snail in HT-29 cells. Compared to control and NDRG2/ΔN groups, NDRG2/FL could obviously shorten the half-life of Snail protein (Figure 5B). Transcriptional factors like Snail are actively degraded through the ubiquitin-proteosome pathway, which clues us to observe the degradation of Snail with proteasome inhibitor MG132. As expected, the Snail suppression by NDRG2 was almost completely reversed by MG132 treatment (Figure 5C), strongly supporting NDRG2 might promote Snail degradation through ubiquitin-proteosome pathway.

FBXO11 was confirmed as the crucial E3 ligase contributing to Snail ubiquitylation and subsequent degradation(28). Nextly, we evaluated whether NDRG2 promoted the ubiquitylation of Snail through FBXO11 pathway. As the immunoprecipitation assay shown in Figure 5D, NDRG2/FL could directly interact with FBXO11 and both of NDRG2 ΔN and ΔC truncations abolished this interaction. Most importantly, forced NDRG2/FL obviously strengthened the E3 ligase FBXO11 targeted

to Snail (Figure 5E) and further promoted Snail ubiquitination (Figure 5F). Our data demonstrated that NDRG2 could enhance E3 ligase FBXO11 with its substrate Snail to induce Ub-mediated degradation of Snail, finally augmented E-cadherin expression.

NDRG2 loss in intestinal epithelial cells increases colitis-associated colorectal cancer. To further evaluate the role of *Ndrg2* in colitis-associated tumor development, mice were subjected to AOM intraperitoneal injection followed with three cycle of DSS-H_2O rotation treatment, and developed colorectal carcinoma (Figure 6A). Then the mice were sacrificed and colon tissues were collected. After the treatment of AOM/DSS, both WT and *Ndrg2*$^{-/-}$ mice developed colon tumors mainly in the distal to middle colon, and the *Ndrg2*$^{-/-}$ mice showed increased tumor numbers and size compared with the WT (Figure 6B). This phenotype was confirmed by HE staining as typical cancerization was observed on distal colon tissue slides (Figure 6C). To further analyze the carcinoma formation in WT and *Ndrg2*$^{-/-}$ mice, we calculated the distribution, number and size of tumors and observed significant increasing of tumors located in the middle and terminal colon (Figure 6D). Meanwhile, the number of tumors with all volume scales (under 2 mm, 2-4 mm and above 4 mm) were increased in *Ndrg2*$^{-/-}$ mice (Figure 6E). Our data demonstrated that intestinal *Ndrg2* loss increased susceptibility to colitis-associated tumor development.

NDRG2 down-regulation attenuated E-cadherin expression and enhanced inflammation in human IBD patients

To confirm the role of NDRG2 in clinic IBDs initiation, we further examined whether NDRG2 affected inflammation in human UC and CD patients (Supplementary Table 3). Interestingly, we found that NDRG2 expression was significantly positively correlated with E-cadherin, and negatively correlated with Snail (Figure 7A-C). Most importantly, NDRG2 expression was negatively correlated with inflammation levels and CD68^{+} macrophage recruitment. Higher NDRG2 expression was correlated with reduced inflammation and CD68^{+} macrophage recruitment at inflammatory foci, while decreases in NDRG2 expression enhanced inflammation and CD68^{+} macrophage infiltration (Figure 7A, D, E).

Taken together, our findings suggest that NDRG2 can positively modulate E-cadherin expression and inhibit inflammation and

macrophage infiltration, thus suppressing colonic inflammation and colitis-associated tumor development (Figure 8).

Discussion

The gastrointestinal tract (GI) is chronically exposed to large numbers of foreign antigens, toxic molecules and microorganisms, and the epithelial barrier makes important contributions to GI health(7, 8, 29, 30). Epithelial barrier dysfunction is believed to contribute to inflammatory bowel disease (IBD) initiation and pathogenesis, mainly by damaging tight junctions (TJs) and/or adherens junctions (AJs). Previous reports have demonstrated that AJ and TJ damage is associated with progressive colonic inflammation in human Crohn's disease (CD) and ulcerative colitis (UC) due to increases in the permeability of lipo-polysaccharide (LPS), peptidoglycan and N-formyl-L-methionyl-L-leucyl-L-phenylalanine (fMLP), major bacterial toxic antigens, which diffuse from the gut lumen to the lamina propria(9, 10, 31, 32).

Our study explored for the role of NDRG2 in intestinal inflammation pathogenesis and determined that NDRG2 modulates of AJ expression *via* Snail and E-cadherin signaling regulation *in vivo*. NDRG2 was initially discovered and demonstrated to be a tumor suppressor gene by our group. We found that NDRG2 played roles in cancer, stress responses and other processes by regulating cell proliferation, differentiation and invasion and cytokine production(14, 33). Our previous work confirmed that NDRG2 expression was positively correlated with cancer prognosis, relapses and overall survival and that NDRG2 regulated EMT by controlling E-cadherin expression and participated in TGF-β-induced oncogenesis in late-stage CRC(22, 23). Furthermore, we found that NDRG2 expression was correlated with E-cadherin expression and malignancy, suggesting that NDRG2 regulates E-cadherin(23, 34).

E-cadherin is an important cytomembrane component and controls cell-cell adhesion by conjugating with β-catenin, α-catenin and p120-catenin complexes to modulate the spaces between epithelial cells(35-37). E-cadherin or p120-catenin loss leads to neonatal death in mice due to epithelial barrier breakdown and gut homeostasis disruption(38). A previous study confirmed that E-cadherin loss in intestinal epithelial cells leads to tight junction dysregulation *via* claudin protein

family modulation(13). Our work demonstrated that NDRG2 loss in intestinal epithelial cells attenuated E-cadherin expression but did not disrupt tight junction structure, as determined *via* electron microscopic analysis. Moreover, we also examined the levels of β-catenin and p120-catenin expression to confirm the mechanisms by which adherens junctions are destroyed and observed no significant alterations in β-catenin or p120-catenin expression in *Ndrg2*$^{-/-}$ mice (data not shown), indicating that AJ destruction caused by NDRG2 loss is induced primarily by E-cadherin suppression. Therefore, intestinal NDRG2 deletion decreased E-cadherin expression and destroyed the adherens junctions between epithelial cells, resulting in increased susceptibility to DSS-induced colitis caused by increased epithelial barrier permeability. Noticeably, we further found that intestinal *Ndrg2* loss could obviously promote the colitis-associated tumor development, which is coincident with its tumor suppressor function.

Snail and Slug are believed to be the most important transcription factors that repress E-cadherin expression in various types of solid tumors and tissues(39-41). Our data showed that Snail significantly increased in Ndrg2 deletion IECs, suggesting reduced E-cadherin expression by *Ndrg*2 loss might be mainly through Snail upregulation. Furthermore, we found NDRG2 can decrease the protein stability of Snail. And we firstly demonstrated that NDRG2 could strengthen the interaction of E3 ligase FBXO11 with Snail to promote the ubiquitination and degradation of Snail. Thus, as shown in Figure 5, intestinal *Ndrg*2 deletion disrupts adherens junction structure in the intestinal epithelium by suppressing E-cadherin expression via promoting FBXO11-Snail interaction for Snail ubiquitination and degradation, thus increasing colonic permeability, colitis and colitis-associated tumor development.

Inflammatory cell infiltration plays an important role in IBD(42-44), and we found that NDRG2 loss facilitated inflammatory cell recruitment and was associated with the inflammatory state of in clinical samples of UC patients. Most importantly, we confirmed the positive correlation of NDRG2 with E-cadherin, and negative correlation with Snail in IBD samples. E-cadherin deficiency is associated with exacerbations of acute and chronic inflammation and facilitates regenerative epithelial changes. NDRG2 loss-induced E-cadherin repression leads to pro-inflammatory cytokine production and

perpetuates inflammation-induced increases in intestinal permeability, resulting in a vicious cycle in which barrier dysfunction allows further leakage of luminal contents, thereby triggering an immune response promoting additional leakiness.

Colitis-associated cancer is the subtype of colorectal cancer which is highly associated with inflammatory bowel diseases. Of the signaling pathways, NF-κB plays a key role in colitis-associated cancer development(45-47). In our colitis-associated cancer mouse model with AOM/DSS treatment, we also confirmed the activated NF-κB/p65 signaling. Noticeably, the proliferative signaling expression of p65, Myc and Ki-67 were much higher in *Ndrg2*$^{-/-}$ mice compared with WT group (data not shown), which is coincident with its tumor suppressor function that NDRG2 inhibits the cancer cells proliferation and metastasis(15, 48-50). Thus, on the side, NDRG2 loss causes E-cadherin reduction and adherens junction structure disruption, increases permeability and colitis; on the other side, decreased NDRG2 also activates the proliferative signaling of NF-κB and Myc etc. This dual mechanism of NDRG2 loss promotes the transformation from chronic inflammation to cancer, finally causes colitis-associated colorectal cancer.

In summary, our work confirmed that NDRG2 played important role in colitis initiation and pathogenesis by regulating AJ structure integrity in normal human colon epithelium. NDRG2 induces E-cadherin expression and enhances AJ structure, protecting the host from foreign antigens to keep gut homeostasis. However, decreases in NDRG2 expression resulted in attenuated E-cadherin expression and AJ structure disruption, finally promoting the colitis and colitis-associated tumor development. Thus, NDRG2 might be an important diagnosis and prognosis marker of colitis and colitis-associated colorectal cancer.

Methods

Mice. Intestine-specific *Ndrg2* knockout mice (*Ndrg2*$^{-/-}$) were generated by Shanghai Biomodel Organism Science & Technology Development Co., Ltd and maintained on a C57BL6/J background. All animals were raised under specific pathogen-free conditions, and 6-to-8-week-old mice were used for the experiments. The wild-type (WT) and *Ndrg2*$^{-/-}$ mice were age-matched, and all the mice that were used in the experiments were male. Typically, at least 8 mice were included each treatment group, and all experiments were

repeated at least three times.

Induction of Colitis and Colitis-associated Colorectal Cancer. To induce colitis, we treated 6-to-8-week-old male mice with 3% DSS (w/v, MW 36 - 50 kDa; MP Biomedicals, Solon, OH) in drinking water for 5 days, followed by DSS-free water for another 5 days, before sacrificing the mice and evaluating their inflammatory responses. Distal colon were obtained for histological analysis, and IECs and LPCs were separated with the total colon. To induce the colitis-associated colorectal cancer, we used the combination of carcinogen AOM with repeated treatment of DSS in drinking water. Mice were treated with intraperitoneally injection with a single dose of AOM (12 mg/kg). After 3 days, 2% DSS dissolving in the drinking water were given for 6 days (the DSS solution was refreshed at day 3), followed by 15 days of regular drinking water. The DSS treatment was repeated for another two cycles. Mice were sacrificed 100 days after AOM injection, colons were removed and the colon tumors were dissected for further analysis.

Histological Score Determination. Distal colonic tissue segments were fixed in 4% neutral-buffered formalin, embedded in paraffin, cut into 8 μm-thick sections, and stained with H&E to histopathologically detect cell hyperplasia, epithelial damage, and inflammatory cell infiltration and to perform histological scoring, which was completed using the following scale: 0: no evidence of inflammation; 1: low-level inflammation; 2: moderate inflammation; 3: high-level inflammation and 4: maximal inflammation.

RNA Isolation and Quantitative Real-Time PCR (qPCR). Total IECs RNA was isolated from healthy and DSS-treated WT and *Ndrg2*$^{-/-}$ mice using Trizol reagent (Takara, Dalian, China), according to the manufacturer's instructions. Primers sequences for quantitative real-time polymerase chain reaction (qRT-PCR) are listed in Supplementary Table 1 and Table 2. qRT-PCR data were analyzed by the $2^{-\Delta\Delta CT}$ method, with *GAPDH* and *β*-actin as the housekeeping gene.

Flow Cytometry Analysis. Flow cytometry analysis was conducted using combinations of IECs and LPCs. Detailed information regarding the staining procedure is available in the supplementary material and methods section.

Co-immunoprecipitation Assay. FLAG tagged NDRG2 (full length and truncated form named as NDRG2/FL, NDRG2/ΔN, NDRG2/ΔC) plasmids were co-transfected with Myc-Snail, HA-FBXO11 (gift from Dr. Yibin Kang, Princeton University) and V5-Ubiquitin or indicated plasmids as described in figures in 60 mm dishes using Lipofectamine 2000 Transfection Reagent (Life Technologies) according to the manufacturer's instructions. For ubiquitination assay, cells were treated with 10 μM MG132 for indicated times after 2 days transfection. Then cells were harvested with lysis buffer (Beyotime, P0013), proteins were quantified using Pierce BCA Protein Assay Kit (Thermo Scientific, 23225) and adjusted to equal concentration. Cell lysates were then immunoprecipitated with primary anti-FLAG (Sigma, F1804) or anti-Myc (CST, 66004) or anti-HA (CST, 3724) or anti-V5 (Sigma, V8137) at 4℃ over night. Then 70 μL protein A/G sepharose (Abcam, ab193262) were added and incubated for 3 hrs. After 3 times washing using NETN wash buffer, Tris 20 mM (pH 8.0), NaCl 100 mM, EDTA 1 mM, NP-40 0.5%, sepharose beads were collected and re-suspended with 70 μL 2xSDS buffer. Pull-down samples and with 5% input were resolved on SDS-PAGE gel and transferred to NC membranes. Then the membranes were detected with appropriate antibodies and visualized using Tanon 6200 Luminescent Imaging Workstation.

Tissue Samples and Immunohistochemistry Staining. This study was approved by the ethics committee of the Fourth Military Medical University. Totally 19 ulcerative colitis cases and 5 Crohn's disease patient samples were obtained from Xijing Hospital from April 2013 to October 2016. The clinical information was shown in Supplementary Table 3. The immunohistochemistry staining of IBD samples was performed as described previously(23).

Statistical Analysis. Differences in parametric data were evaluated using Student's t test. *$p<0.05$ and **$p<0.01$ were considered statistically significant.

Study approval. All animal procedures were reviewed and approved by the Animal Care and Use Committee of Fourth Military Medical University. All animals were housed, cared for, and used in compliance with the

Guide for the Care and Use of Laboratory Animals. All patients in the disease sample cohort provided full consent for the study.

Acknowledgments

This work was supported by the National Natural Science Foundation of China (No. 81770523, 31571437, 81672751), the Founds for Creative Research Groups of China (No. 81421003), and the State Key Laboratory of Cancer Biology Project (CBSKL201406, CBSKL2017Z08 and CBSKL2017Z11).

Author contributions

JZ designed the overall project and developed the hypothesis. MYW, YZM and LLS conducted the experiments, analyzed the data and wrote the manuscript. YZM and MYW collected the colonic tissues. YQX, ZSL and ZW made the pathological diagnoses. YZM, LJL and XB generated the human colorectal cancer NDRG2 knockout cells. HYQ assisted with the flow cytometry and data analyses. KCW and LBY contributed to the experimental design and provided the reagents. All authors participated in the revision of the manuscript and agreed with the final version to be submitted. JZ supervised the overall project.

References

1. Pastorelli L, De Salvo C, Mercado JR, Vecchi M, and Pizarro TT. Central role of the gut epithelial barrier in the pathogenesis of chronic intestinal inflammation: lessons learned from animal models and human genetics. *Frontiers in immunology.* 2013;4:280.
2. Arrieta MC, Bistritz L, and Meddings JB. Alterations in intestinal permeability. *Gut.* 2006;55(10):1512-20.
3. Kostic AD, Xavier RJ, and Gevers D. The microbiome in inflammatory bowel disease: current status and the future ahead. *Gastroenterology.* 2014;146(6):1489-99.
4. Wellman AS, Metukuri MR, Kazgan N, Xu X, Xu Q, Ren NSX, et al. Intestinal Epithelial Sirtuin 1 Regulates Intestinal Inflammation During Aging in Mice by Altering the Intestinal Microbiota. *Gastroenterology.* 2017;153(3):772-86.
5. Rescigno M, and Di Sabatino A. Dendritic cells in intestinal homeostasis and disease. *The Journal of clinical investigation.* 2009;119(9):2441-50.
6. Radtke AL, Quayle AJ, and Herbst-Kralovetz MM. Microbial products alter the expression of membrane-associated mucin and antimicrobial peptides in a three-dimensional human endocervical epithelial cell model. *Biology of reproduction.* 2012;87(6):132.
7. Stein J, Ries J, and Barrett KE. Disruption of intestinal barrier function associated with experimental colitis: possible role of mast cells. *The American journal of physiology.* 1998;274(1 Pt 1):G203-9.
8. Taddei A, Giampietro C, Conti A, Orsenigo F, Breviario F, Pirazzoli V, et al. Endothelial adherens junctions control tight junctions by VE-cadherin-mediated upregulation of claudin-5. *Nature cell biology.* 2008;10(8):923-34.
9. Landy J, Ronde E, English N, Clark SK, Hart AL, Knight SC, et al. Tight junctions in inflammatory bowel diseases and inflammatory bowel disease associated colorectal cancer. *World journal of gastroenterology.* 2016;22(11):3117-26.
10. Schulzke JD, Ploeger S, Amasheh M, Fromm A, Zeissig S, Troeger H, et al. Epithelial tight junctions in intestinal inflammation. *Annals of the New York Academy of Sciences.* 2009;1165:294-300.
11. Smalley-Freed WG, Efimov A, Burnett PE, Short SP, Davis MA, Gumucio DL, et al. p120-catenin is essential for maintenance of barrier function and intestinal homeostasis in mice. *The Journal of clinical investigation.* 2010;120(6):1824-35.
12. Grill JI, Neumann J, Hiltwein F, Kolligs FT, and Schneider MR. Intestinal E-cadherin Deficiency Aggravates Dextran Sodium Sulfate-Induced Colitis. *Digestive diseases and sciences.* 2015;60(4):895-902.
13. Bondow BJ, Faber ML, Wojta KJ, Walker EM, and Battle MA. E-cadherin is required for intestinal morphogenesis in the mouse. *Dev Biol.* 2012;371(1):1-12.
14. Yao L, Zhang J, and Liu X. NDRG2: a Myc-repressed gene involved in cancer and cell stress. *Acta biochimica et biophysica Sinica.* 2008;40(7):625-35.
15. Deng Y, Yao L, Chau L, Ng SS, Peng Y, Liu X, et al. N-Myc downstream-regulated gene 2 (NDRG2) inhibits glioblastoma cell proliferation. *Int J Cancer.* 2003;106(3):342-7.
16. Xu X, Li J, Sun X, Guo Y, Chu D, Wei L, et al. Tumor suppressor NDRG2 inhibits glycolysis and glutaminolysis in colorectal cancer cells by repressing c-Myc expression. *Oncotarget.* 2015;6(28):26161-76.
17. Zhang J, Li F, Liu X, Shen L, Liu J, Su J, et al. The repression of human differentiation-related gene NDRG2 expression by Myc via Miz-1-dependent

interaction with the NDRG2 core promoter. *J Biol Chem.* 2006;281(51):39159-68.

18. Lorentzen A, Vogel LK, Lewinsky RH, Saebo M, Skjelbred CF, Godiksen S, et al. Expression of NDRG2 is down-regulated in high-risk adenomas and colorectal carcinoma. *BMC Cancer.* 2007;7:192.
19. Kim YJ, Yoon SY, Kim JT, Song EY, Lee HG, Son HJ, et al. NDRG2 expression decreases with tumor stages and regulates TCF/beta-catenin signaling in human colon carcinoma. *Carcinogenesis.* 2009;30(4):598-605.
20. Kim YJ, Yoon SY, Kim JT, Choi SC, Lim JS, Kim JH, et al. NDRG2 suppresses cell proliferation through down-regulation of AP-1 activity in human colon carcinoma cells. *Int J Cancer.* 2009;124(1):7-15.
21. Shen L, Qu X, Li H, Xu C, Wei M, Wang Q, et al. NDRG2 facilitates colorectal cancer differentiation through the regulation of Skp2-p21/p27 axis. *Oncogene.* 2018.
22. Chu D, Zhang Z, Li Y, Wu L, Zhang J, Wang W, et al. Prediction of colorectal cancer relapse and prognosis by tissue mRNA levels of NDRG2. *Molecular cancer therapeutics.* 2011;10(1):47-56.
23. Shen L, Qu X, Ma Y, Zheng J, Chu D, Liu B, et al. Tumor suppressor NDRG2 tips the balance of oncogenic TGF-beta via EMT inhibition in colorectal cancer. *Oncogenesis.* 2014;3:e86.
24. Feng T, Qin H, Wang L, Benveniste EN, Elson CO, and Cong Y. Th17 cells induce colitis and promote Th1 cell responses through IL-17 induction of innate IL-12 and IL-23 production. *J Immunol.* 2011;186(11):6313-8.
25. Lindemans CA, Calafiore M, Mertelsmann AM, O'Connor MH, Dudakov JA, Jenq RR, et al. Interleukin-22 promotes intestinal-stem-cell-mediated epithelial regeneration. *Nature.* 2015;528(7583):560-4.
26. Tanaka H, Takechi M, Kiyonari H, Shioi G, Tamura A, and Tsukita S. Intestinal deletion of Claudin-7 enhances paracellular organic solute flux and initiates colonic inflammation in mice. *Gut.* 2015;64(10):1529-38.
27. Wheeler JM, Kim HC, Efstathiou JA, Ilyas M, Mortensen NJ, and Bodmer WF. Hypermethylation of the promoter region of the E-cadherin gene (CDH1) in sporadic and ulcerative colitis associated colorectal cancer. *Gut.* 2001;48(3):367-71.
28. Zheng H, Shen M, Zha YL, Li W, Wei Y, Blanco MA, et al. PKD1 phosphorylation-dependent degradation of SNAIL by SCF-FBXO11 regulates epithelial-mesenchymal transition and metastasis. *Cancer Cell.* 2014;26(3):358-73.
29. Nusrat A, Sitaraman SV, and Neish A. Interaction of bacteria and bacterial toxins with intestinal epithelial cells. *Current gastroenterology reports.* 2001;3(5):392-8.
30. Peterson LW, and Artis D. Intestinal epithelial cells: regulators of barrier function and immune homeostasis. *Nature reviews Immunology.* 2014;14(3):141-53.
31. Kobayashi K, Oyama S, Numata A, Rahman MM, and Kumura H. Lipopolysaccharide disrupts the milk-blood barrier by modulating claudins in mammary alveolar tight junctions. *PloS one.* 2013;8(4):e62187.
32. Guo M, Yuan SY, Frederich BJ, Sun C, Shen Q, McLean DL, et al. Role of non-muscle myosin light chain kinase in neutrophil-mediated intestinal barrier dysfunction during thermal injury. *Shock.* 2012;38(4):436-43.
33. Guo YJ, Liu JX, and Guan YW. Hypoxia induced upregulation of miR-301a/b contributes to increased cell autophagy and viability of prostate cancer cells by targeting NDRG2. *European review for medical and pharmacological sciences.* 2016;20(1):101-8.

34. Kim YJ, Kang HB, Yim HS, Kim JH, and Kim JW. NDRG2 positively regulates E-cadherin expression and prolongs overall survival in colon cancer patients. *Oncology reports.* 2013;30(4):1890-8.
35. Morton RA, Ewing CM, Nagafuchi A, Tsukita S, and Isaacs WB. Reduction of E-cadherin levels and deletion of the alpha-catenin gene in human prostate cancer cells. *Cancer research.* 1993;53(15):3585-90.
36. Bulgakova NA, and Brown NH. Drosophila p120-catenin is crucial for endocytosis of the dynamic E-cadherin-Bazooka complex. *Journal of cell science.* 2016;129(3):477-82.
37. Orsulic S, Huber O, Aberle H, Arnold S, and Kemler R. E-cadherin binding prevents beta-catenin nuclear localization and beta-catenin/LEF-1-mediated transactivation. *Journal of cell science.* 1999;112 (Pt 8):1237-45.
38. Sumagin R, and Parkos CA. Epithelial adhesion molecules and the regulation of intestinal homeostasis during neutrophil transepithelial migration. *Tissue barriers.* 2015;3(1-2):e969100.
39. Batlle E, Sancho E, Franci C, Dominguez D, Monfar M, Baulida J, et al. The transcription factor snail is a repressor of E-cadherin gene expression in epithelial tumour cells. *Nature cell biology.* 2000;2(2):84-9.
40. Yokoyama K, Kamata N, Hayashi E, Hoteiya T, Ueda N, Fujimoto R, et al. Reverse correlation of E-cadherin and snail expression in oral squamous cell carcinoma cells in vitro. *Oral oncology.* 2001;37(1):65-71.
41. Hajra KM, Chen DY, and Fearon ER. The SLUG zinc-finger protein represses E-cadherin in breast cancer. *Cancer research.* 2002;62(6):1613-8.
42. Stevceva L, Pavli P, Husband AJ, and Doe WF. The inflammatory infiltrate in the acute stage of the dextran sulphate sodium induced colitis: B cell response differs depending on the percentage of DSS used to induce it. *BMC clinical pathology.* 2001;1(1):3.
43. Koelink PJ, Overbeek SA, Braber S, Morgan ME, Henricks PA, Abdul Roda M, et al. Collagen degradation and neutrophilic infiltration: a vicious circle in inflammatory bowel disease. *Gut.* 2014;63(4):578-87.
44. Hanauer SB. Inflammatory bowel disease: epidemiology, pathogenesis, and therapeutic opportunities. *Inflamm Bowel Dis.* 2006;12 Suppl 1:S3-9.
45. Karin M. NF-kappaB as a critical link between inflammation and cancer. *Cold Spring Harbor perspectives in biology.* 2009;1(5):a000141.
46. Grivennikov SI, Greten FR, and Karin M. Immunity, inflammation, and cancer. *Cell.* 2010;140(6):883-99.
47. Greten FR, Eckmann L, Greten TF, Park JM, Li ZW, Egan LJ, et al. IKKbeta links inflammation and tumorigenesis in a mouse model of colitis-associated cancer. *Cell.* 2004;118(3):285-96.
48. Park S, Oh SS, Lee KW, Lee YK, Kim NY, Kim JH, et al. NDRG2 contributes to cisplatin sensitivity through modulation of BAK-to-Mcl-1 ratio. *Cell Death Dis.* 2018;9(2):30.
49. Nakahata S, Ichikawa T, Maneesaay P, Saito Y, Nagai K, Tamura T, et al. Loss of NDRG2 expression activates PI3K-AKT signalling via PTEN phosphorylation in ATLL and other cancers. *Nature communications.* 2014;5:3393.
50. Tamura T, Ichikawa T, Nakahata S, Kondo Y, Tagawa Y, Yamamoto K, et al. Loss of NDRG2 Expression Confers Oral Squamous Cell Carcinoma with Enhanced Metastatic Potential. *Cancer Res.* 2017;77(9):2363-74.

Figure legends

Figure 1. Intestine-specific conditional *Ndrg2* knockout mice (*Ndrg2*$^{-/-}$) exhibited increased susceptibility to dextran sodium sulfate (DSS)-induced colitis. (A) Western blotting analysis for Ndrg2 in intestinal epithelial cells (IECs) from WT and *Ndrg2*$^{-/-}$ mice (n=2/group). **(B)** Quantitative real-time PCR (qRT-PCR) for *Ndrg2* in IECs from WT and *Ndrg2*$^{-/-}$ mice (n=3/group; **p<0.01). **(C-H)** WT and *Ndrg2*$^{-/-}$ mice on a C57BL/6 background were subjected to **(C-G)** 3% DSS treatment (n=15/group) or **(H)** 4% DSS treatment (n=15/group) to induce colitis. **(C)** Body weights and **(D, E)** colon lengths on day 10 in the WT and *Ndrg2*$^{-/-}$ mice with and without DSS treatment. **(F)** Representative H&E-staining showing the colonic sections and **(G)** the DAI scores of the WT and *Ndrg2*$^{-/-}$ mice on days 0, 5, 7 and 10 of 3% DSS administration. **(H)** Survival rate analysis. Data **(C, D, G)** are represented as the mean ± SEM. *p<0.05, **p<0.01 (Student's t test).

Figure 2. ***Ndrg2* deficiency enhanced inflammation in intestinal epithelial cells (IECs) characterized by increased inflammatory cytokine and chemokine expression in the setting of dextran sodium sulfate (DSS)-induced colitis (n=12/group)**. WT and *Ndrg2*$^{-/-}$ mice on a C57BL/6 background were treated with 3% DSS (n=12/group). Flow cytometry analysis was performed on days 0 and 10 after DSS treatment. **(A)** CD11b+ stained monocytes, CD11b^{+} F4/80^{+} stained macrophages, CD11b^{+} Gr-1^{+} stained neutrophils, and CD11b^{+} Siglec-F^{+} stained eosinophils. **(B)** Monocyte, macrophage, neutrophil and eosinophil percentages on day 0 and **(C)** day 10. **(D)** Quantitative real-time PCR (qRT-PCR) for the expression of the pro-inflammatory chemokines *CXCL-1, CXCL-2* and *CCL-5*; **(E)** pro-inflammatory cytokines *IL-1β* and *TNF-α*, and anti-inflammatory cytokines *IL-10*. Data are represented as the mean ± SEM. *p<0.05, **p<0.01, n.s., no significance (Student's t test).

Figure 3. *Ndrg2* deficiency enhanced lipopolysaccharide (LPS)-induced inflammation. (A) Detection of serum LPS concentrations in WT and *Ndrg2*$^{-/-}$ mice with and without 3% DSS treatment (n=6/group). **(B-D)** WT and *Ndrg2*$^{-/-}$ mice were treated with 1 g/mL ampicillin for 1 week before LPS administration. **(B)** Detection of serum LPS levels in WT and *Ndrg2*$^{-/-}$ mice with

0.1 mg/kg LPS treatment (n=4/group). **(C, D)** Quantitative real-time PCR (qRT-PCR) for *IL-1β, IL-6, TNF-α, CXCL-1 and CXCL-2* expression in the IECs of WT and *Ndrg2*$^{-/-}$ mice treated with 0.1 mg/kg LPS (n=4/group). Data are represented as the mean ± SEM. *p<0.05, n.s., no significance.

Figure 4. *Ndrg2* deletion disrupted adherens junctions (AJs) integrity in the colonic epithelium. (A) Intestinal permeability was measured by determining serum FITC-dextran concentrations (40 KD and 500 KD dextran respectively) in the presence and absence of 3% DSS treatment (n=8/group). **(B)** Adherens junction (AJ) detection in the colonic epithelium of WT and *Ndrg2*$^{-/-}$ mice via electron microscopy (n=6/group). **(C)** AJ distances in the colonic epithelium of WT and *Ndrg2*$^{-/-}$ mice (n=6/group). **(D)** Immunofluorescence micrographs for NDRG2 (green) and E-cadherin (red) expression in the colons of WT and *Ndrg2*$^{-/-}$ mice (n=6/group). **(E)** Western blotting detection for E-cadherin, Snail, Slug and NDRG2 expression in the IECs of WT and *Ndrg2*$^{-/-}$ mice (left panel, n=4/group). Right panel is the band intensity quantification of E-cadherin and Snail respectively. **(A, C, E)** Data are represented as the mean ± SEM. *p<0.05, **p<0.01, n.s., no significance.

Figure 5. NDRG2 augmented E-cadherin expression *via* promoting the ubiquitylation and degradation of Snail. (A) Endogenous E-cadherin and Snail protein level in full length NDRG2 (NDRG2/FL), N-terminal truncation (NDRG2/ΔN) and C-terminal truncation (NDRG2/ΔC) stably overexpression HT-29 cell lines (Left); Graphical representation of NDRG2/FL, NDRG2/ΔN and NDRG2/ΔC truncation mutants (Right). **(B)** Under treatment of CHX (100 μg/ml) for indicated time, NDRG2/FL and NDRG2/ΔN stably overexpressed HT-29 cells lysate were subjected to a CHX pulse-chase assay. Western blotting data were quantified using ImageJ software. Bottom panel (curve) was the quantification data of Snail protein. **(C)** NDRG2/FL and NDRG2/ΔN stably overexpressed HT-29 cells were treated with 10 μM MG132, and cells were harvested at the indicated time points. Western blotting was employed to test endogenous Snail protein expression level. **(D)** HEK293T cells were co-transfected with plasmids expressing HA-FBXO11, FLAG-NDRG2/FL, FLAG-NDRG2/ΔN and FLAG-NDRG2/ΔC as indicated respectively, with EGFP as control. The cell lysate was immunoprecipitated with FLAG antibody or an immunoglobulin G (IgG) control and subjected to western blotting analysis. **(E)** HEK293T cells were co-transfected with

plasmids expressing HA-FBXO11 and Myc-Snail with either EGFP or FLAG-NDRG2/FL as indicated respectively. Cell lysates were immunoprecipitated with anti-HA antibody, and the interaction of FBXO11 and Snail was detected with anti-Myc antibody. **(F)** HEK293T cells were co-transfected with plasmids expressing HA-FBXO11, Myc-Snail and V5-Ubiquitin together, with either EGFP or FLAG-NDRG2/FL. Cells were treated with 10 μM MG132 for 6 hrs before cell lysates were immunoprecipitated with anti-FLAG antibody, and the poly-ubiquitylated Snail protein was detected by anti-V5 antibody.

Figure 6. Intestinal deletion of *Ndrg*2 enhanced the initiation and progression of AOM-DSS induced colorectal carcinoma. (A) Method of the treatment of AOM-DSS in our study. **(B)** Colons with tumors between WT and *Ndrg2*$^{-/-}$ after AOM-DSS treatment. **(C)** HE staining of normal epithelium and AOM-DSS induced colorectal carcinoma in WT and *Ndrg2*$^{-/-}$ mice. Bar: 100 μm. **(D)** Analysis of tumor numbers from the whole, middle and distal colons between WT and *Ndrg2*$^{-/-}$ mice respectively. **(E)** Analysis of tumor numbers with small size (<2 mm), middle size (2-4 mm) and big size (>4 mm) from the whole colon between WT and *Ndrg2*$^{-/-}$ mice respectively. WT: n=24; *Ndrg2*$^{-/-}$: n=26. *p<0.05, **p<0.01.

Figure 7. **NDRG2 positively correlated with E-cadherin and negatively correlated with Snail and inflammation in human ulcerative colitis patients. (A)** Immunolocalization of NDRG2, E-cadherin, Snail, CD68^{+} and HE staining on human ulcerative colitis (UC) tissues. In UC slides, immunohistochemistry assay showed the representative case with mild, moderate and sever inflammation degree. Scale bar, 100 μm. **(B-E)** Linear regression and Pearson's correlation analysis of NDRG2 with inflammation degree, E-cadherin and Snail in UC and CD samples respectively.

Figure 8. A schematic for the role of NDRG2 regulating Snail, E-cadherin and adherens junction structure integrity in DSS-induced colitis. Intestinal NDRG2 loss disrupts AJs structure in the colonic epithelium by suppressing E-cadherin expression via promotion Snail ubiquitination and degradation, thus increasing colonic permeability, colitis and colitis-associated tumor development in Ndrg2-/- mice.

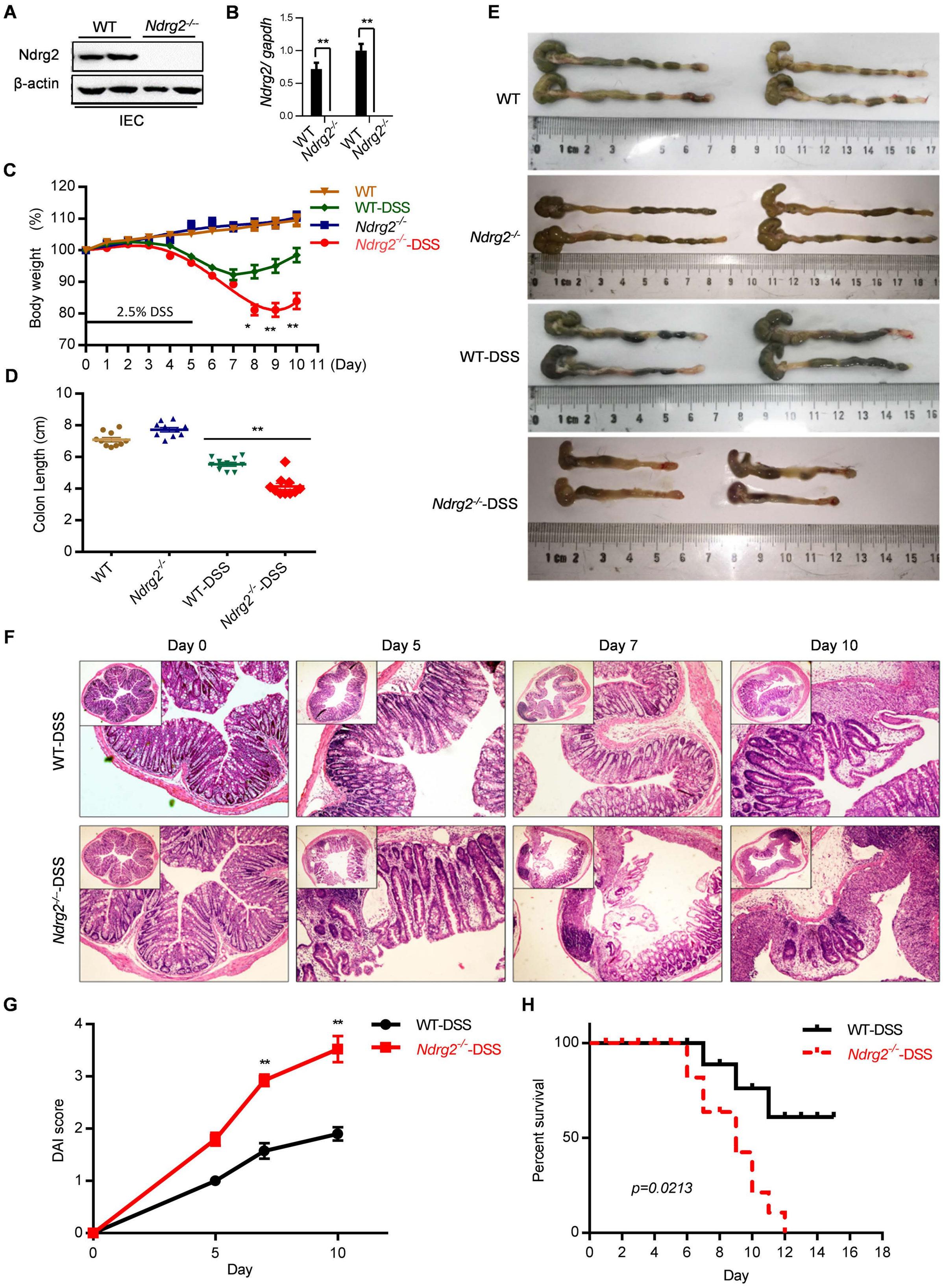
A
WT
Ndrg2-/-
Ndrg2
β-actin
IEC
B
Ndrg2/ gapdh
1.5
1.0
0.5
0.0
**
**
WT
Ndrg2-/-
WT
Ndrg2-/-
C
Body weight (%)
120
110
100
90
80
70
2.5% DSS
*
**
**
0 1 2 3 4 5 6 7 8 9 10 11 (Day)
WT
WT-DSS
Ndrg2-/-
Ndrg2-/--DSS
D
Colon Length (cm)
10
8
6
4
2
0
**
WT
Ndrg2-/-
WT-DSS
Ndrg2-/- -DSS
E
WT
Ndrg2-/-
WT-DSS
Ndrg2-/--DSS
F
Day 0
Day 5
Day 7
Day 10
WT-DSS
Ndrg2-/--DSS
G
DAI score
4
3
2
1
0
**
**
0
5
10
Day
WT-DSS
Ndrg2-/--DSS
H
Percent survival
100
50
0
p=0.0213
0 2 4 6 8 10 12 14 16 18
Day
WT-DSS
Ndrg2-/--DSS

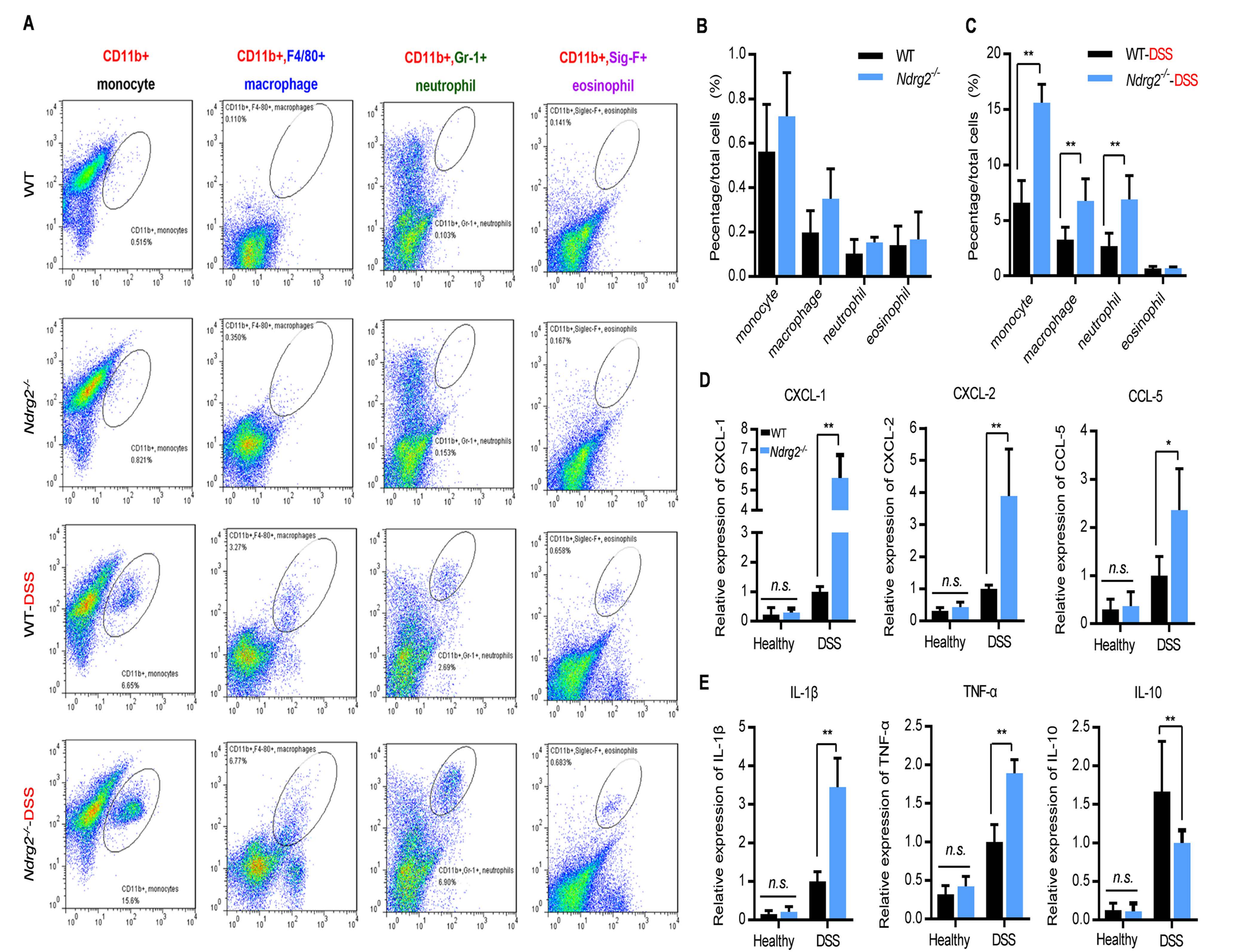
A
CD11b+
monocyte
CD11b+,F4/80+
macrophage
CD11b+,Gr-1+
neutrophil
CD11b+,Sig-F+
eosinophil
WT
Ndrg2-/-
WT-DSS
Ndrg2-/--DSS
CD11b+, monocytes 0.515%
CD11b+, F4-80+, macrophages 0.110%
CD11b+, Gr-1+, neutrophils 0.103%
CD11b+,Siglec-F+, eosinophils 0.141%
CD11b+, monocytes 0.821%
CD11b+, F4-80+, macrophages 0.350%
CD11b+, Gr-1+, neutrophils 0.153%
CD11b+,Siglec-F+, eosinophils 0.167%
CD11b+, monocytes 6.65%
CD11b+,F4-80+, macrophages 3.27%
CD11b+,Gr-1+, neutrophils 2.69%
CD11b+,Siglec-F+, eosinophils 0.658%
CD11b+, monocytes 15.6%
CD11b+,F4-80+, macrophages 6.77%
CD11b+,Gr-1+, neutrophils 6.90%
CD11b+,Siglec-F+, eosinophils 0.683%
B
Pecentage/total cells (%)
WT
Ndrg2-/-
monocyte
macrophage
neutrophil
eosinophil
C
Pecentage/total cells (%)
WT-DSS
Ndrg2-/--DSS
**
D
CXCL-1
CXCL-2
CCL-5
Relative expression of CXCL-1
Relative expression of CXCL-2
Relative expression of CCL-5
n.s.
*
Healthy
DSS
E
IL-1β
TNF-α
IL-10
Relative expression of IL-1β
Relative expression of TNF-α
Relative expression of IL-10

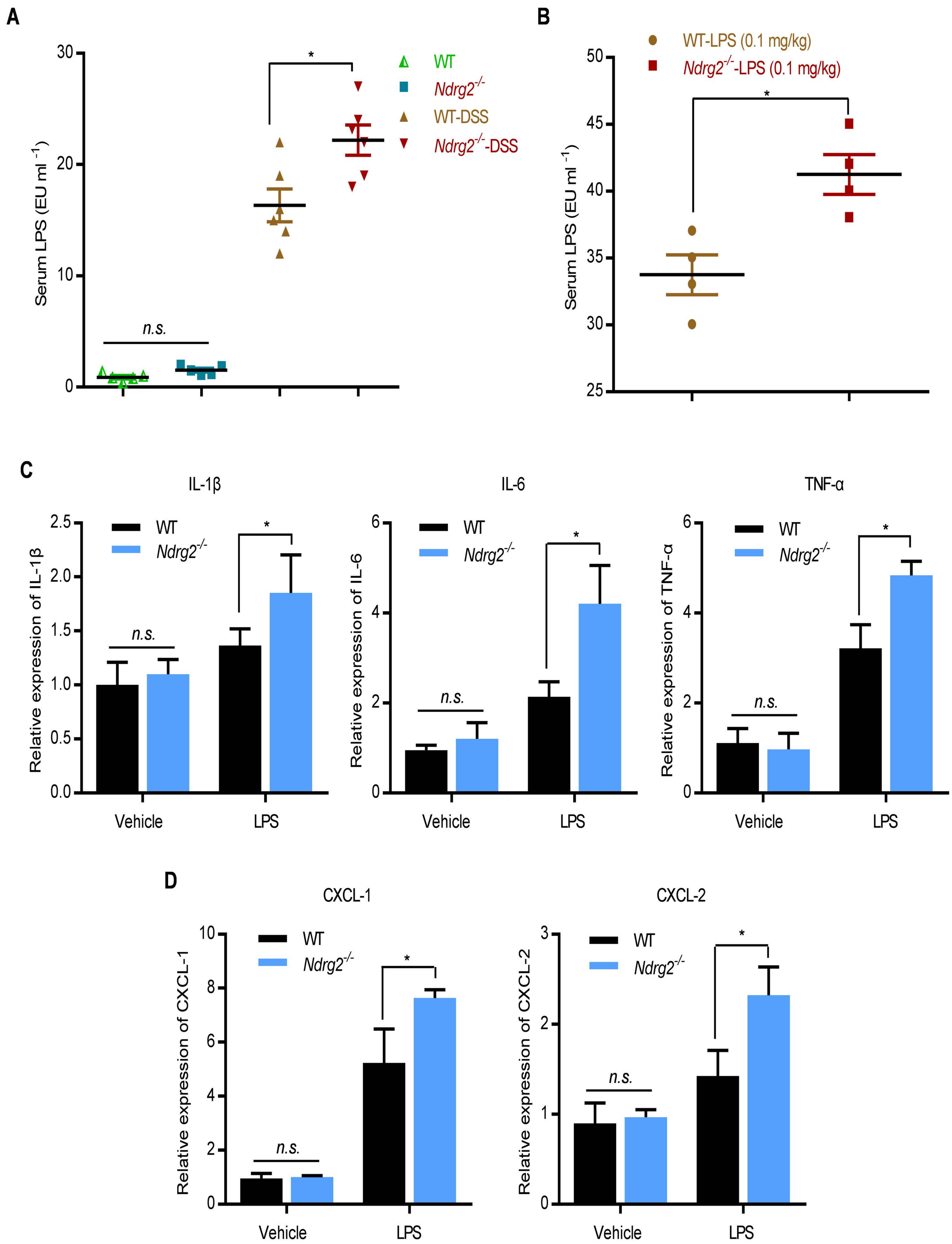
A
Serum LPS (EU ml -1)
30
20
10
0
*
n.s.
WT
Ndrg2-/-
WT-DSS
Ndrg2-/--DSS
B
WT-LPS (0.1 mg/kg)
Ndrg2-/--LPS (0.1 mg/kg)
Serum LPS (EU ml -1)
50
45
40
35
30
25
*
C
IL-1β
IL-6
TNF-α
Relative expression of IL-1β
Relative expression of IL-6
Relative expression of TNF-α
WT
Ndrg2-/-
n.s.
*
Vehicle
LPS
D
CXCL-1
CXCL-2
Relative expression of CXCL-1
Relative expression of CXCL-2
WT
Ndrg2-/-
n.s.
*
Vehicle
LPS

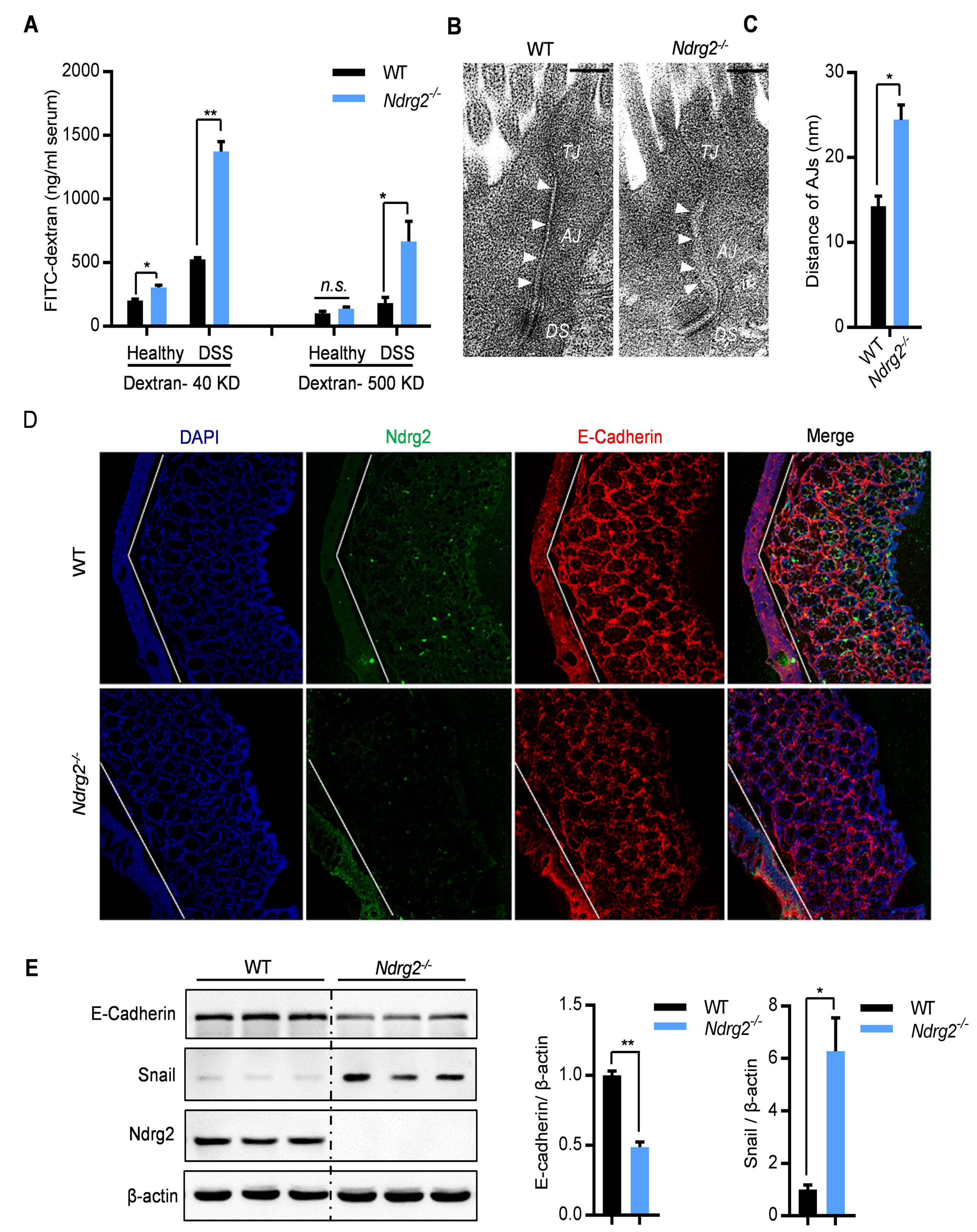
A
FITC-dextran (ng/ml serum)
2000
1500
1000
500
0
WT
Ndrg2-/-
**
*
n.s.
*
Healthy
DSS
Healthy
DSS
Dextran- 40 KD
Dextran- 500 KD
B
WT
Ndrg2-/-
TJ
AJ
DS
TJ
AJ
DS
C
Distance of AJs (nm)
30
20
10
0
*
WT
Ndrg2-/-
D
DAPI
Ndrg2
E-Cadherin
Merge
WT
Ndrg2-/-
E
WT
Ndrg2-/-
E-Cadherin
Snail
Ndrg2
β-actin
E-cadherin/ β-actin
1.5
1.0
0.5
0.0
**
WT
Ndrg2-/-
Snail / β-actin
8
6
4
2
0
*
WT
Ndrg2-/-

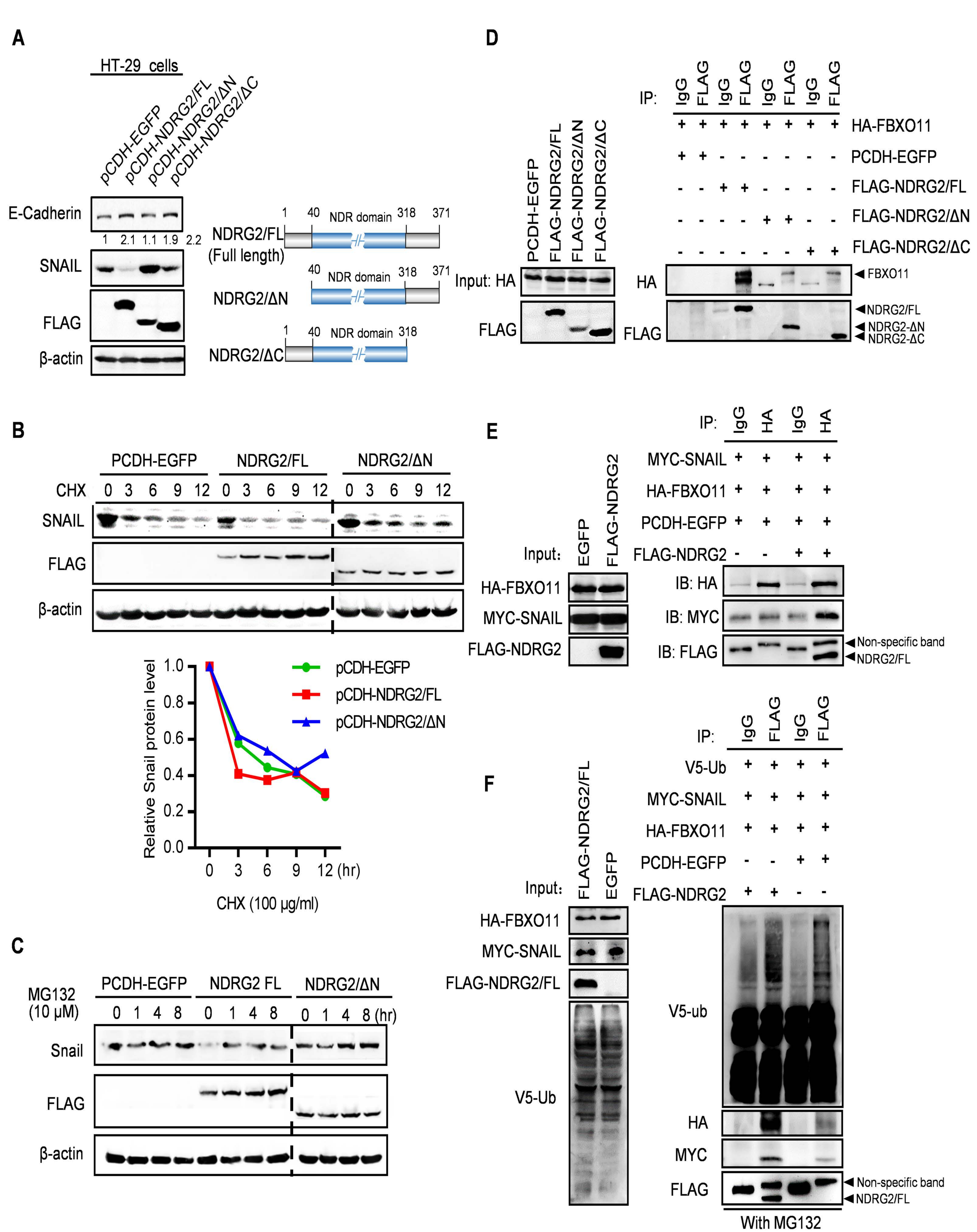
A
HT-29 cells
pCDH-EGFP
pCDH-NDRG2/FL
pCDH-NDRG2/ΔN
pCDH-NDRG2/ΔC
E-Cadherin
1 2.1 1.1 1.9 2.2
SNAIL
FLAG
β-actin
NDRG2/FL (Full length)
NDRG2/ΔN
NDRG2/ΔC
NDR domain
1 40 318 371
B
PCDH-EGFP
NDRG2/FL
NDRG2/ΔN
CHX 0 3 6 9 12 0 3 6 9 12 0 3 6 9 12
SNAIL
FLAG
β-actin
Relative Snail protein level
1.0
0.8
0.6
0.4
0.2
0.0
0 3 6 9 12 (hr)
CHX (100 μg/ml)
pCDH-EGFP
pCDH-NDRG2/FL
pCDH-NDRG2/ΔN
C
MG132 (10 μM)
PCDH-EGFP
NDRG2 FL
NDRG2/ΔN
0 1 4 8 0 1 4 8 0 1 4 8 (hr)
Snail
FLAG
β-actin
D
PCDH-EGFP
FLAG-NDRG2/FL
FLAG-NDRG2/ΔN
FLAG-NDRG2/ΔC
Input: HA
FLAG
IP: IgG FLAG IgG FLAG IgG FLAG IgG FLAG
HA-FBXO11 + + + + + + + +
PCDH-EGFP + + - - - - - -
FLAG-NDRG2/FL - - + + - - - -
FLAG-NDRG2/ΔN - - - - + + - -
FLAG-NDRG2/ΔC - - - - - - + +
HA
FLAG
FBXO11
NDRG2/FL
NDRG2-ΔN
NDRG2-ΔC
E
Input:
EGFP
FLAG-NDRG2
HA-FBXO11
MYC-SNAIL
FLAG-NDRG2
IP: IgG HA IgG HA
MYC-SNAIL + + + +
HA-FBXO11 + + + +
PCDH-EGFP + + + +
FLAG-NDRG2 - - + +
IB: HA
IB: MYC
IB: FLAG
Non-specific band
NDRG2/FL
F
Input:
FLAG-NDRG2/FL
EGFP
HA-FBXO11
MYC-SNAIL
FLAG-NDRG2/FL
V5-Ub
IP: IgG FLAG IgG FLAG
V5-Ub + + + +
MYC-SNAIL + + + +
HA-FBXO11 + + + +
PCDH-EGFP - - + +
FLAG-NDRG2 + + - -
V5-ub
HA
MYC
FLAG
Non-specific band
NDRG2/FL
With MG132

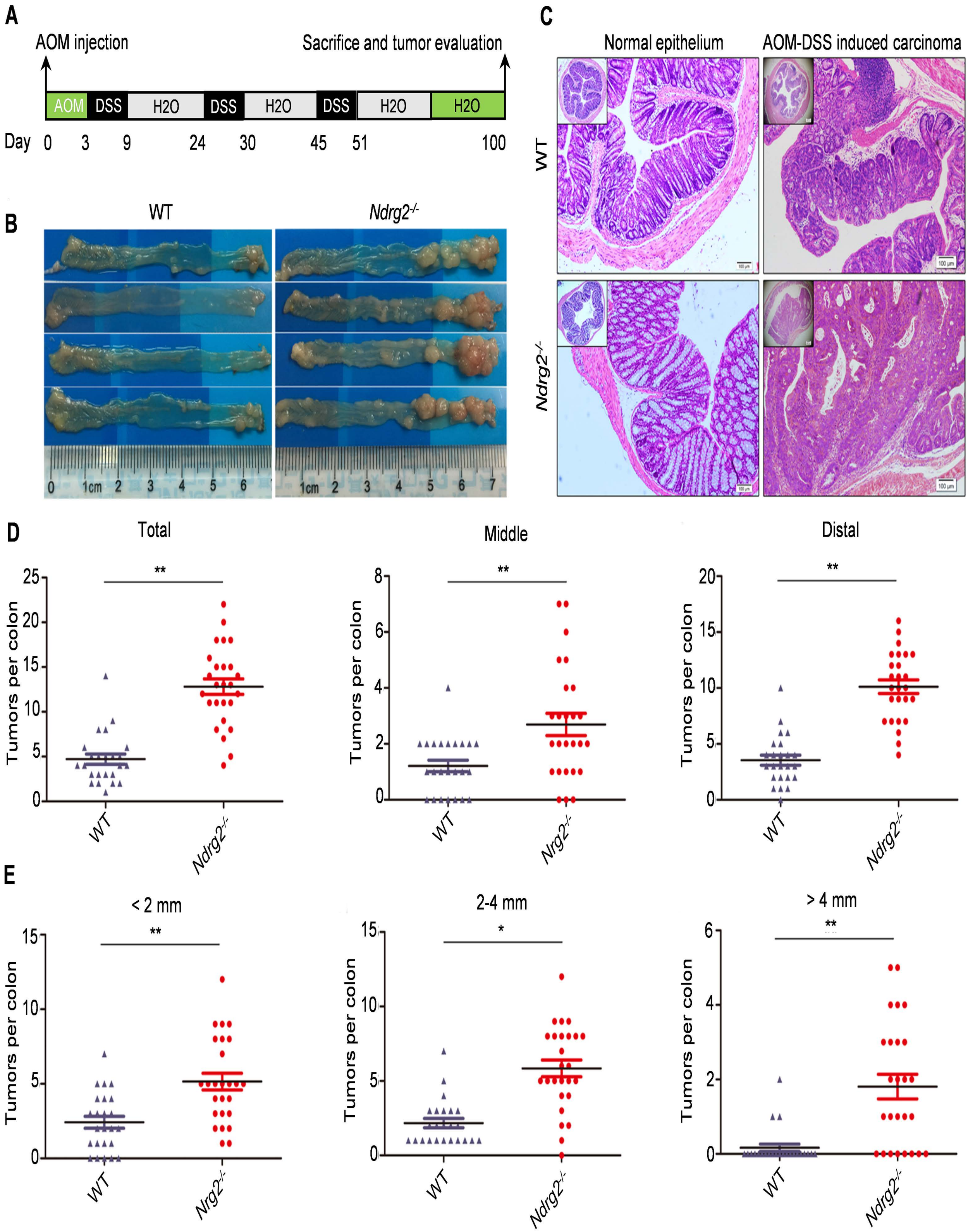
A
AOM injection
Sacrifice and tumor evaluation
AOM
DSS
H2O
DSS
H2O
DSS
H2O
H2O
Day 0 3 9 24 30 45 51 100
B
WT
Ndrg2-/-
C
Normal epithelium
AOM-DSS induced carcinoma
WT
Ndrg2-/-
D
Total
Middle
Distal
Tumors per colon
**
WT
Ndrg2-/-
Nrg2-/-
E
< 2 mm
2-4 mm
> 4 mm
*

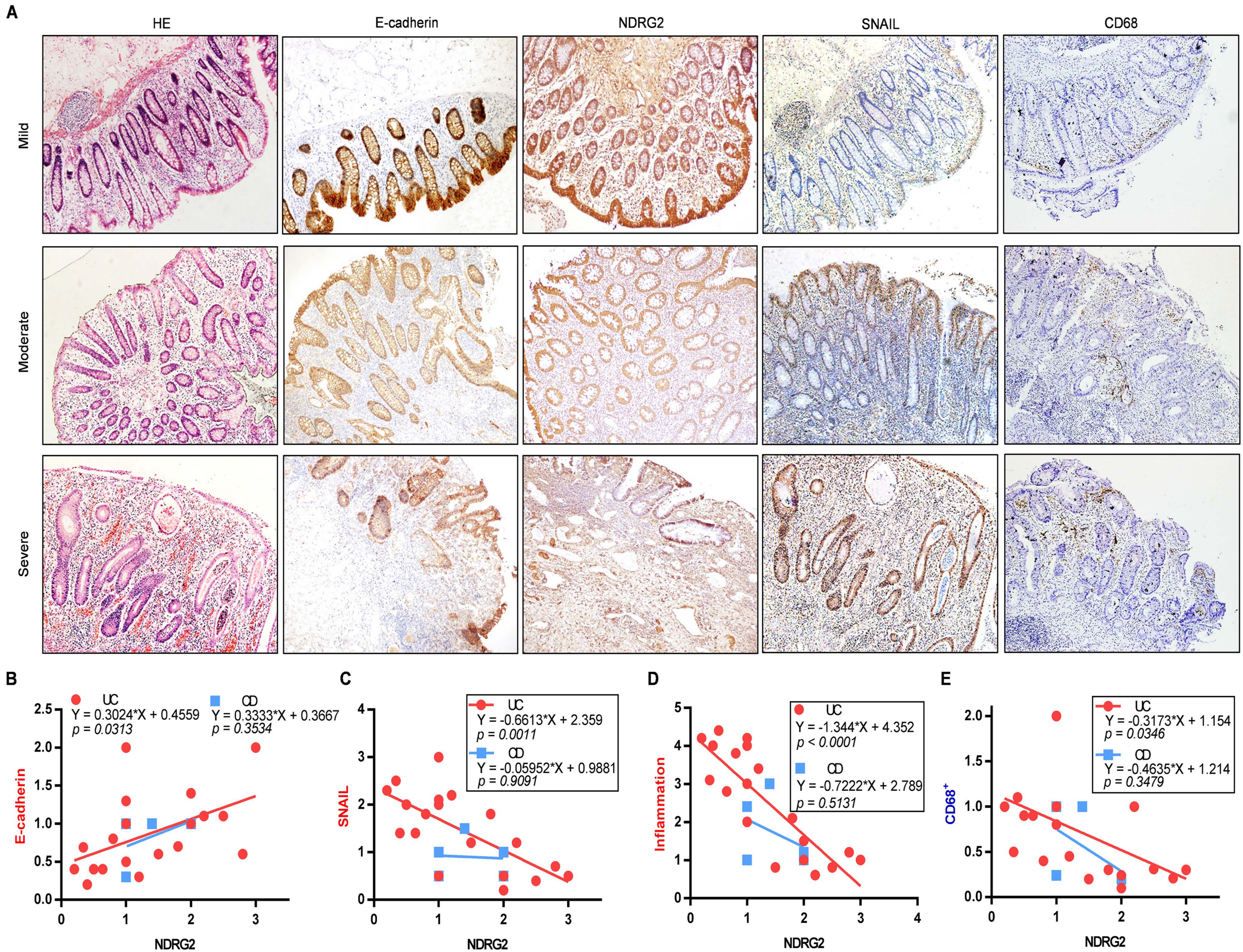
A
HE
E-cadherin
NDRG2
SNAIL
CD68
Mild
Moderate
Severe
B
UC
Y = 0.3024*X + 0.4559
p = 0.0313
CD
Y = 0.3333*X + 0.3667
p = 0.3534
E-cadherin
NDRG2
C
UC
Y = -0.6613*X + 2.359
p = 0.0011
CD
Y = -0.05952*X + 0.9881
p = 0.9091
SNAIL
NDRG2
D
UC
Y = -1.344*X + 4.352
p < 0.0001
CD
Y = -0.7222*X + 2.789
p = 0.5131
Inflammation
NDRG2
E
UC
Y = -0.3173*X + 1.154
p = 0.0346
CD
Y = -0.4635*X + 1.214
p = 0.3479
CD68+
NDRG2

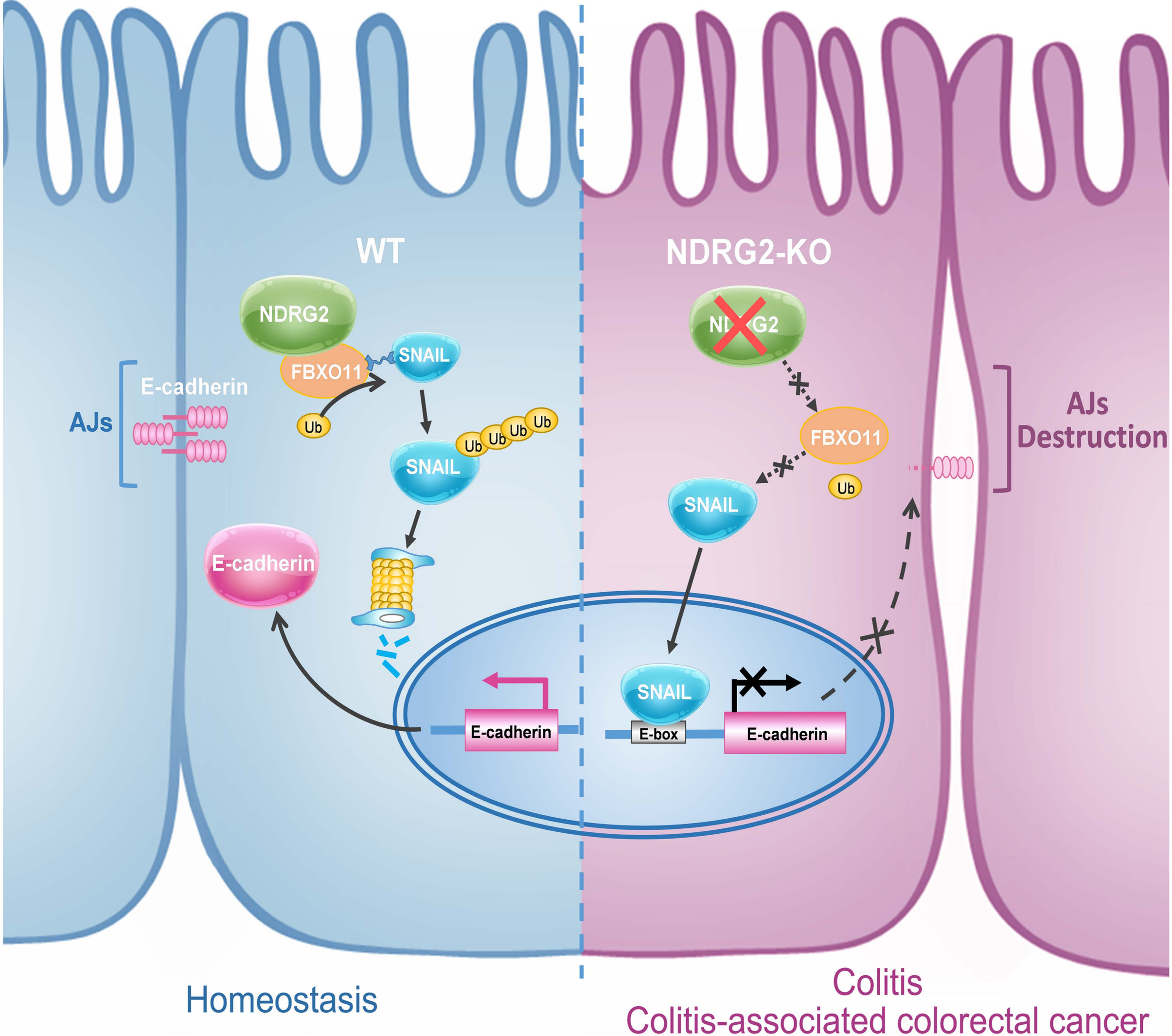
WT
NDRG2-KO
NDRG2
FBXO11
SNAIL
Ub
E-cadherin
AJs
SNAIL
Ub
Ub
Ub
Ub
E-cadherin
E-cadherin
NDRG2
FBXO11
Ub
SNAIL
AJs
Destruction
SNAIL
E-box
E-cadherin
Homeostasis
Colitis
Colitis-associated colorectal cancer

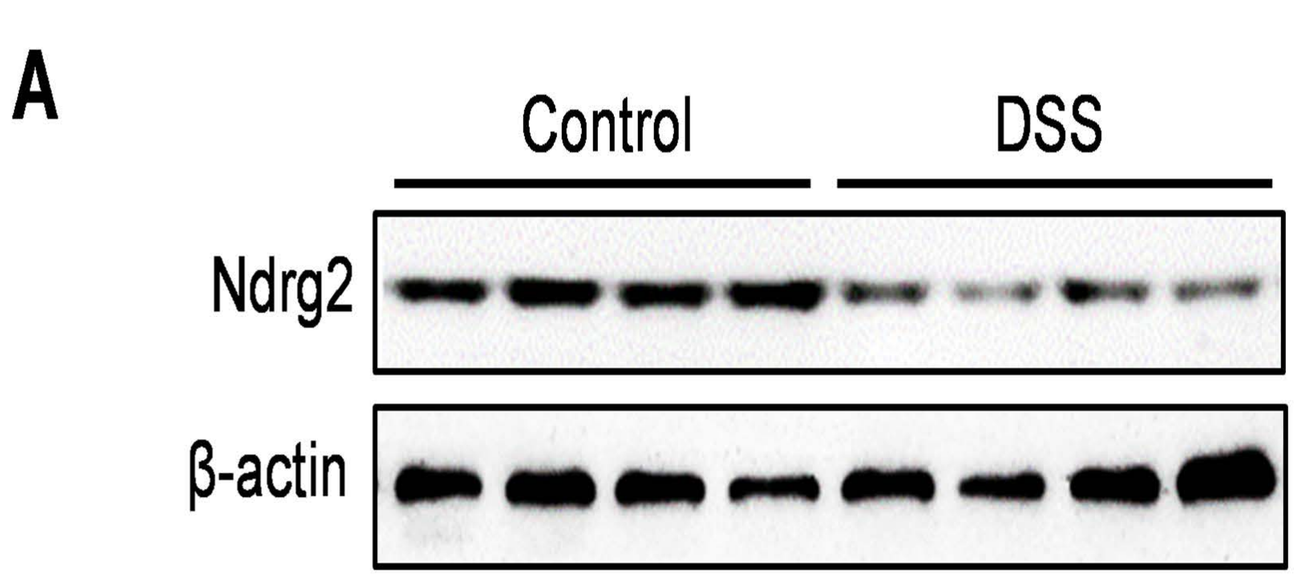
A
Control
DSS
Ndrg2
β-actin

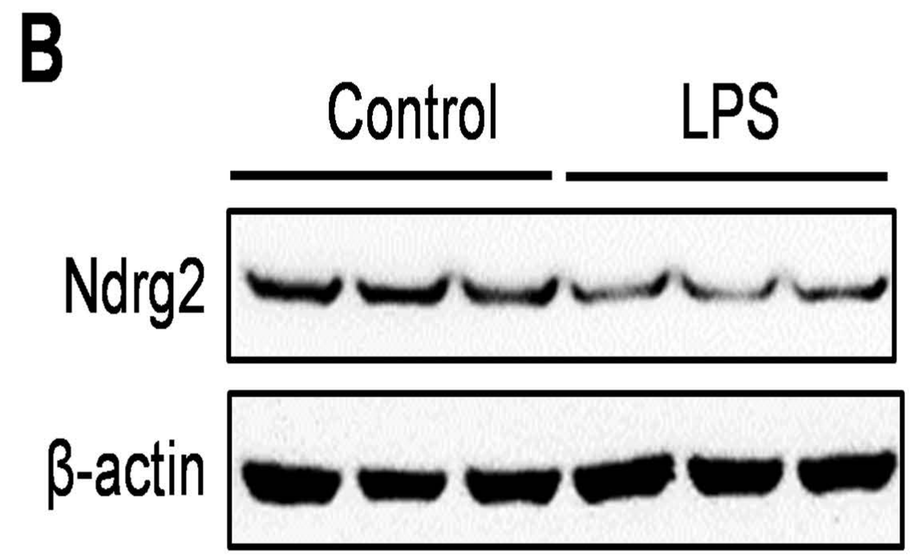
B
Control
LPS
Ndrg2
β-actin

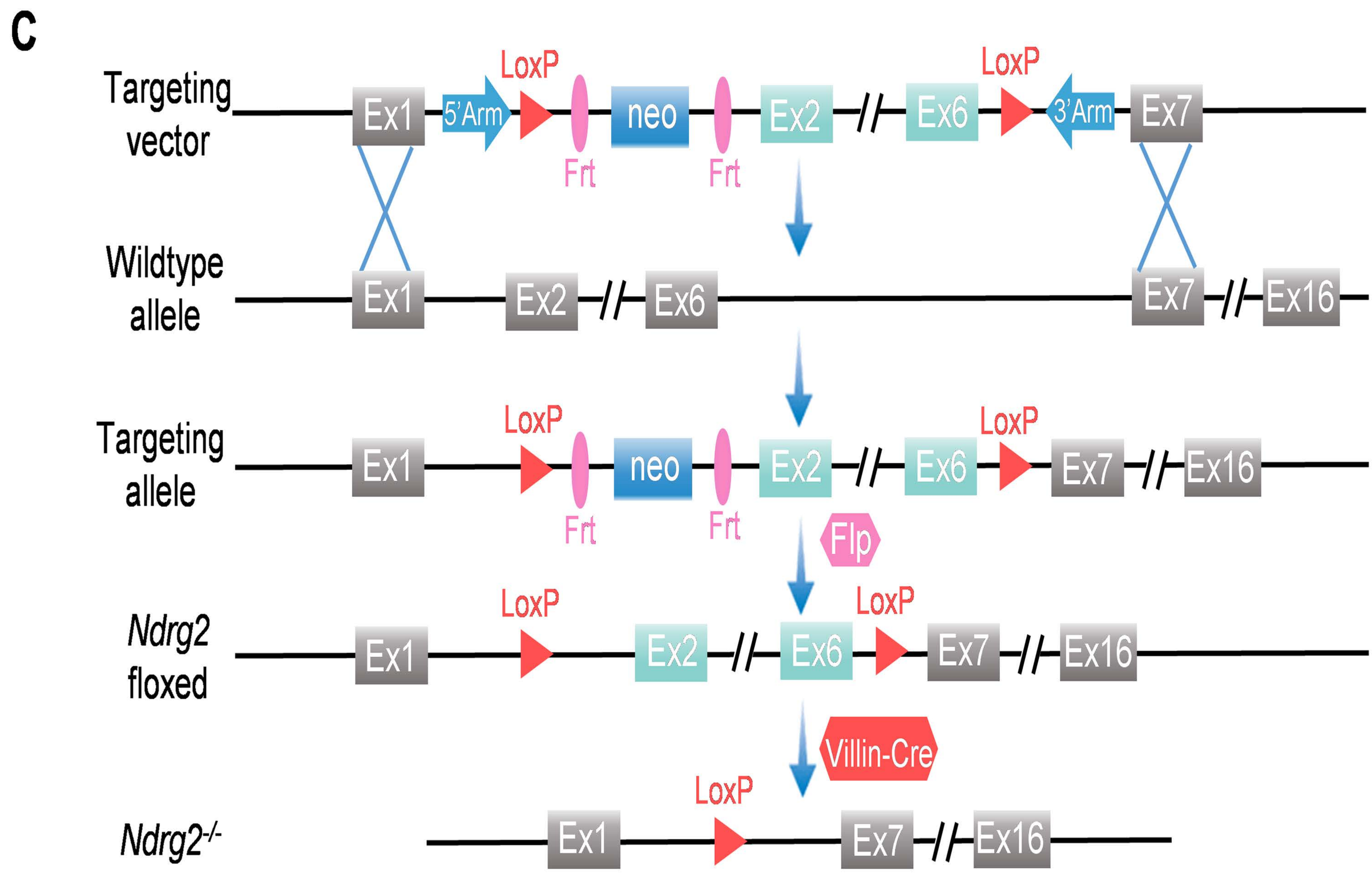
C
Targeting vector
Ex1
5'Arm
LoxP
Frt
neo
Frt
Ex2
Ex6
LoxP
3'Arm
Ex7
Wildtype allele
Ex1
Ex2
Ex6
Ex7
Ex16
Targeting allele
Ex1
LoxP
Frt
neo
Frt
Ex2
Ex6
LoxP
Ex7
Ex16
Flp
Ndrg2 floxed
Ex1
LoxP
Ex2
Ex6
LoxP
Ex7
Ex16
Villin-Cre
Ndrg2-/-
Ex1
LoxP
Ex7
Ex16

D
WT
Ndrg2-/-

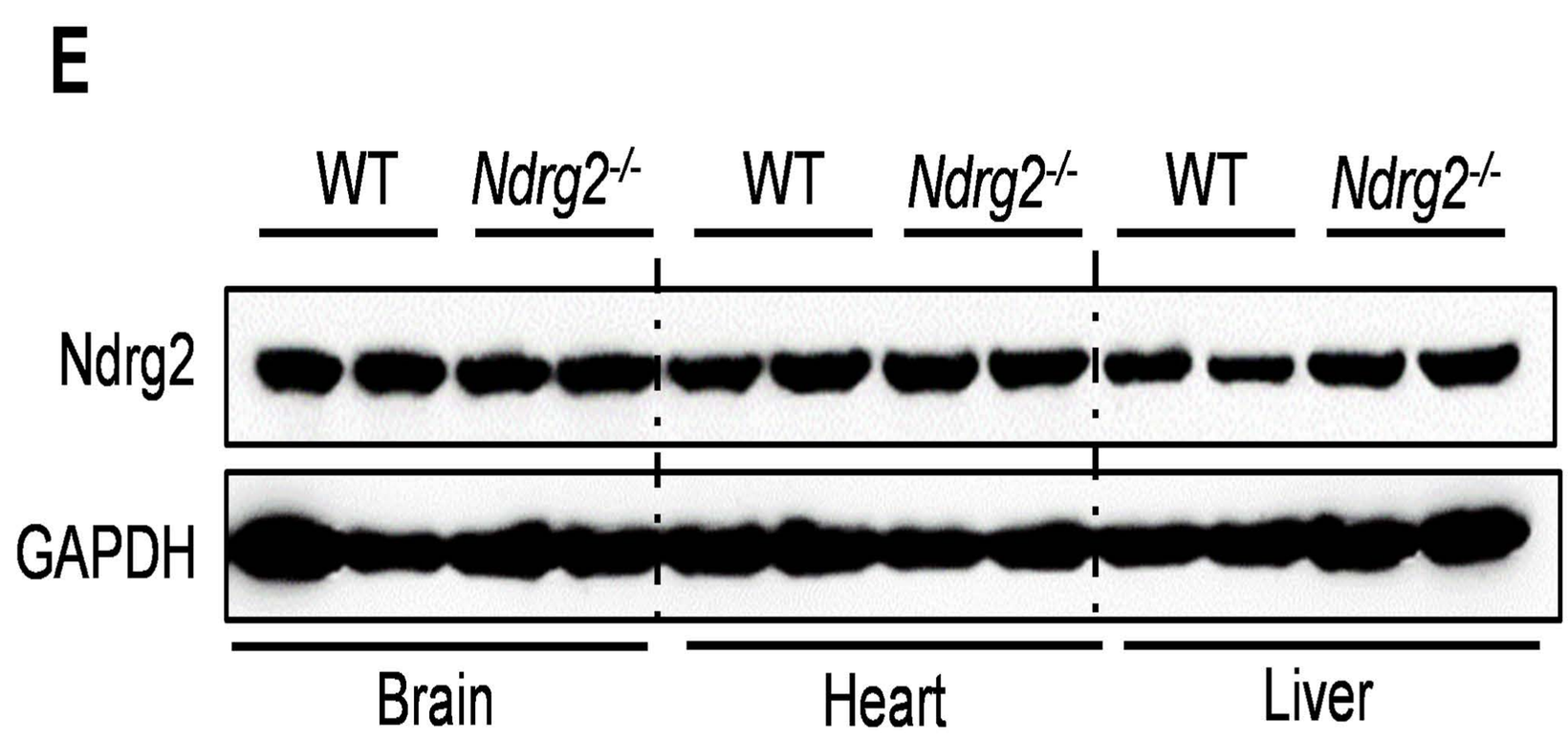
E
WT
Ndrg2-/-
WT
Ndrg2-/-
WT
Ndrg2-/-
Ndrg2
GAPDH
Brain
Heart
Liver

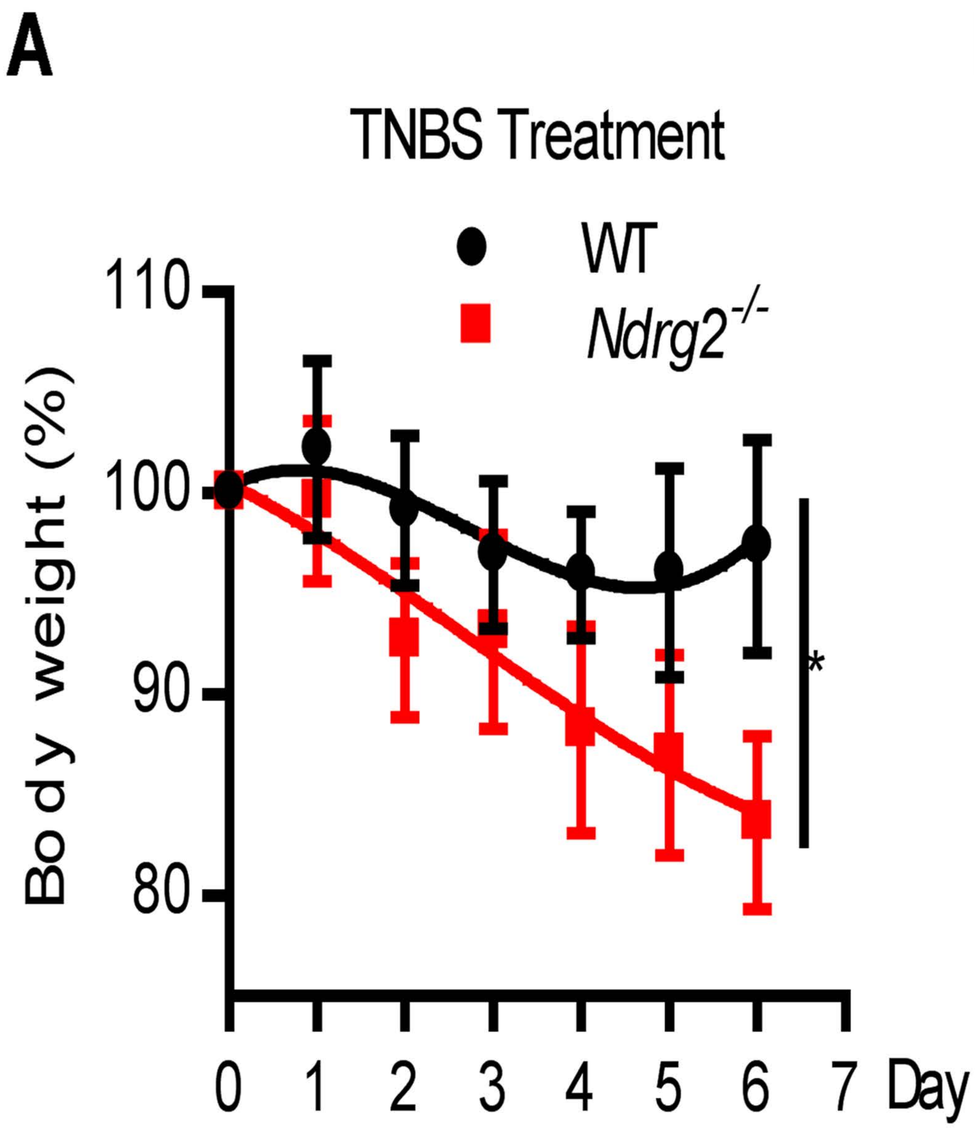
A
TNBS Treatment
WT
Ndrg2-/-
Body weight (%)
110
100
90
80
0 1 2 3 4 5 6 7 Day
*

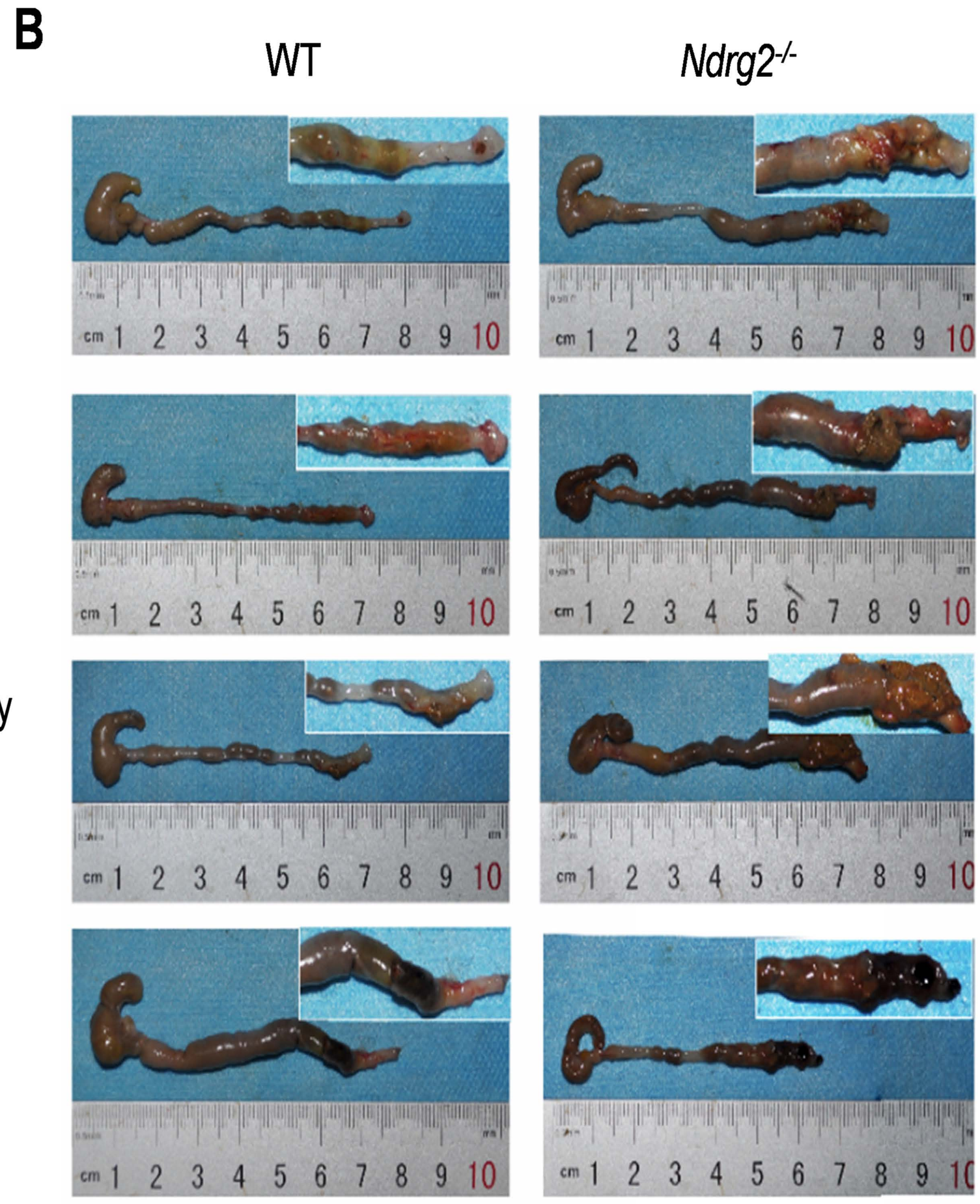
B
WT
Ndrg2-/-
cm 1 2 3 4 5 6 7 8 9 10

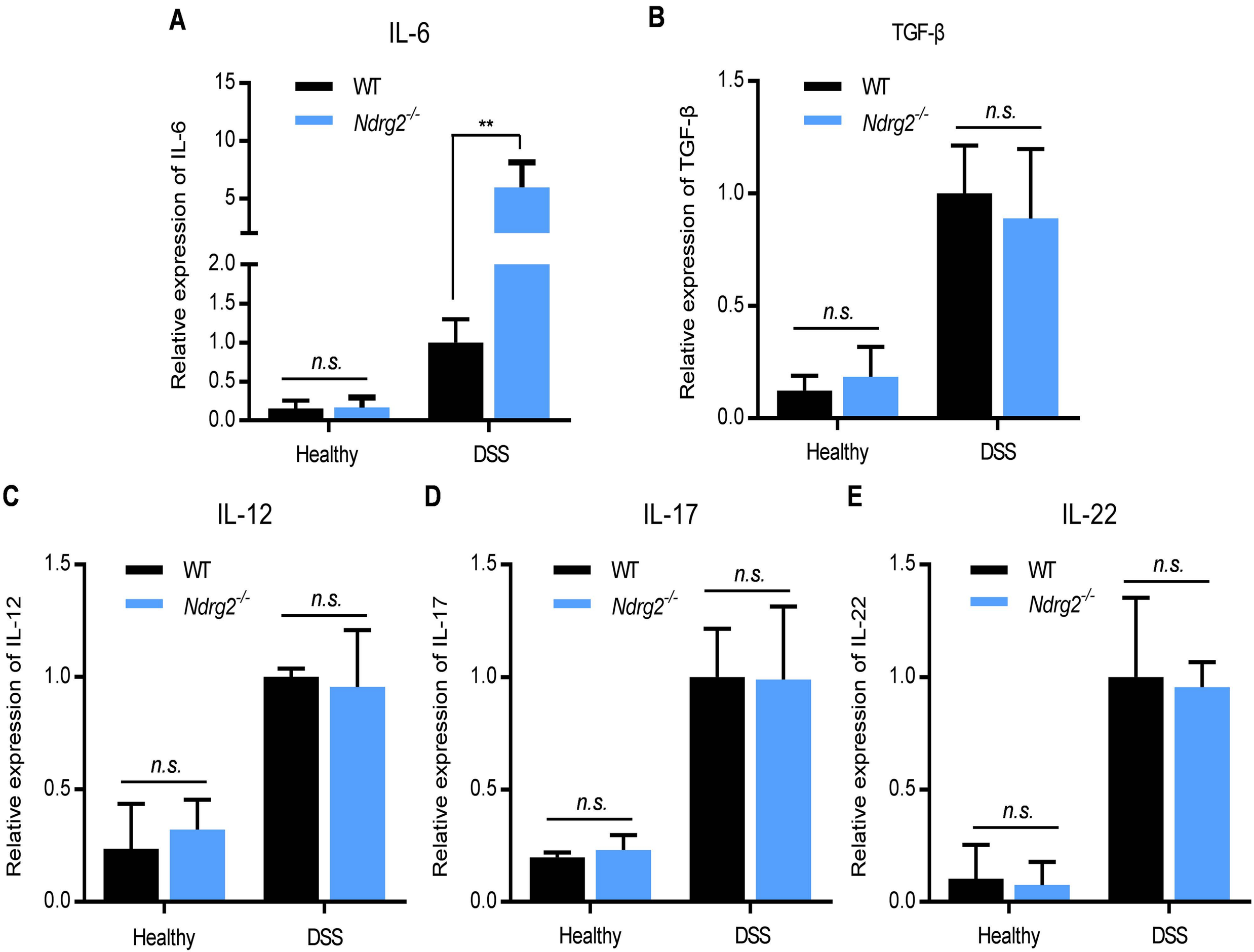
A
IL-6
WT
Ndrg2-/-
Relative expression of IL-6
15
10
5
2.0
1.5
1.0
0.5
0.0
**
n.s.
Healthy
DSS
B
TGF-β
WT
Ndrg2-/-
Relative expression of TGF-β
1.5
1.0
0.5
0.0
n.s.
n.s.
Healthy
DSS
C
IL-12
WT
Ndrg2-/-
Relative expression of IL-12
1.5
1.0
0.5
0.0
n.s.
n.s.
Healthy
DSS
D
IL-17
WT
Ndrg2-/-
Relative expression of IL-17
1.5
1.0
0.5
0.0
n.s.
n.s.
Healthy
DSS
E
IL-22
WT
Ndrg2-/-
Relative expression of IL-22
1.5
1.0
0.5
0.0
n.s.
n.s.
Healthy
DSS

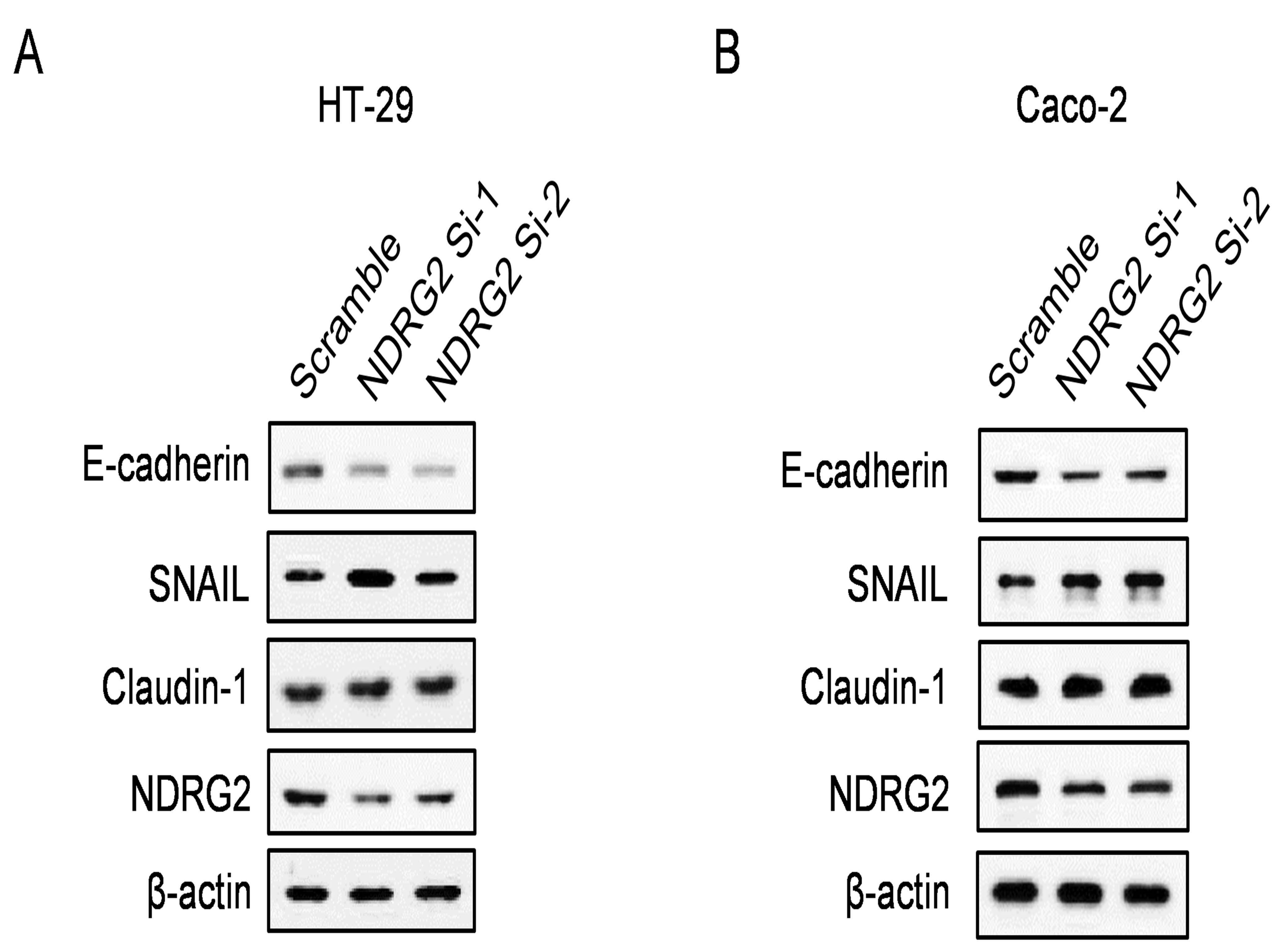
A
HT-29
Scramble
NDRG2 Si-1
NDRG2 Si-2
E-cadherin
SNAIL
Claudin-1
NDRG2
β-actin
B
Caco-2
Scramble
NDRG2 Si-1
NDRG2 Si-2
E-cadherin
SNAIL
Claudin-1
NDRG2
β-actin